Liquefaction Potential in the Central Mississippi Valley

U.S. GEOLOGICAL SURVEY BULLETIN 1832

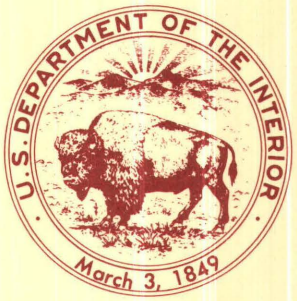

Liquefaction Potential in the Central Mississippi Valley

By STEPHEN F. OBERMEIER

U.S. GEOLOGICAL SURVEY BULLETIN 1832

DEPARTMENT OF THE INTERIOR
DONALD PAUL HODEL, Secretary

U.S. GEOLOGICAL SURVEY
Dallas L. Peck, Director

UNITED STATES GOVERNMENT PRINTING OFFICE: 1988

For sale by the Books and Open-File Reports Section,
U.S. Geological Survey, Federal Center,
Box 25425, Denver, CO 80225

Library of Congress Cataloging in Publication Data
Obermeier, Stephen F.
Liquefaction potential in the central Mississippi Valley
(U.S. Geological Survey bulletin ; 1832)
Bibliography: p.
1. Soil mechanics—Mississippi River Valley. 2. Soil liquefaction—Mississippi River Valley. I. Title. II. Series.
QE75.B9 no. 1832 624.1'5136 88–600375
[TA710.3.M74]

CONTENTS

FIGURES

TABLES

Liquefaction Potential in the Central Mississippi Valley

By Stephen F. Obermeier

Abstract

Liquefaction-induced ground failure caused by the 1811–12 New Madrid earthquakes was commonplace over large areas, even far from the epicenters. Recurrence of strong earthquakes in the New Madrid seismic zone (which lies near the middle of the central Mississippi Valley) would undoubtedly cause severe liquefaction again and lead to the destruction of many bridges, buildings, and other constructed works. There is a need to predict, for different earthquake magnitudes, the circumstances under which unconsolidated materials may liquefy.

Estimated accelerations presented in this paper for the 1811–12 earthquakes are based on the pattern of sand blows caused by those earthquakes and mechanical properties of sands. From these acceleration data and from modern seismicity data, accelerations for liquefaction analysis can be estimated for any magnitude earthquake. The Simplified Procedure of Seed and Idriss can then be used to evaluate liquefaction potential. (The terms "liquefaction potential" and "liquefaction susceptibility" are used in the sense defined by T.L. Youd and D.M. Perkins ("Mapping liquefaction-induced ground failure potential," Proceedings of the American Society of Civil Engineers, Journal of the Geotechnical Engineering Division, v. 104, no. GT4, p. 433-446.) Liquefaction susceptibility is largely a measure of material property and indicates the degree of susceptibility to liquefaction (such as low or high) during strong earthquake shaking only. Liquefaction potential describes the level of susceptibility at a site combined with the likelihood that the site will be subjected to earthquake shaking severe enough to trigger liquefaction.) Because of uncertainties in predicting strong earthquake accelerations, another method is also presented. This method, called the magnitude method, is based on occurrences of liquefaction from scattered sites around the world, from the 1811–12 earthquakes, and from other historical earthquakes in the central Mississippi Valley. It is recommended that the level of liquefaction potential be judged on the basis of both the Simplified Procedure of Seed and Idriss and the magnitude method.

Sand and silt deposits in the central Mississippi Valley are the most susceptible to liquefaction. Large areas of terraces and flood plains in the region are underlain by moderately dense to loose clean sands and silty sands. Relating the properties of these deposits to their liquefaction potentials is reasonably easy and straightforward. However, there are also many thick glacial lake deposits, eolian deposits, and reworked eolian deposits made up of silt-rich and clay-bearing materials in the valley. Most of these deposits have low liquefaction susceptibility, but, locally, some may have high susceptibility. Field methods for assessing their properties are crude, and laboratory data are so scarce that no simple guidelines are available for evaluating liquefaction potential. Laboratory tests are needed to supplement field studies for many silt-rich and clay-bearing deposits.

INTRODUCTION

Both historical accounts of the 1811–12 New Madrid earthquakes and present-day evidence show that liquefaction-induced ground failure was very commonplace and widespread in alluvial lowlands, especially between the towns of New Madrid, Mo., and Marked Tree, Ark. (shown in fig. 1). This ground failure was typically manifested by sand blows, lateral spreads, ground fissures, and localized distortion and warping of the ground surface (Fuller, 1912). Many landslides along streams were doubtlessly caused by liquefaction. If the 1811–12 earthquakes were to recur today, liquefaction-induced ground failure would probably make impassable much of the Interstate highway system in the St. Francis Basin (shown in fig. 2) from Cairo, Ill., to nearly as far south as Memphis, Tenn. Many highway bridges would probably be knocked down or badly damaged by lateral spreads or collapse of the stream banks. The pavement would be so damaged by ground fissures and warping that it would be impassable at many places. Many other constructed works would also be damaged. In addition, there might be widespread flooding (Saucier, 1977) owing to venting to the ground surface of liquefied sand and water. Many houses and other structures would also be destroyed by the effects of liquefaction.

Recounting what took place in 1811–12 and what would take place today, given the recurrence of strong earthquakes, makes it clear that liquefaction would be

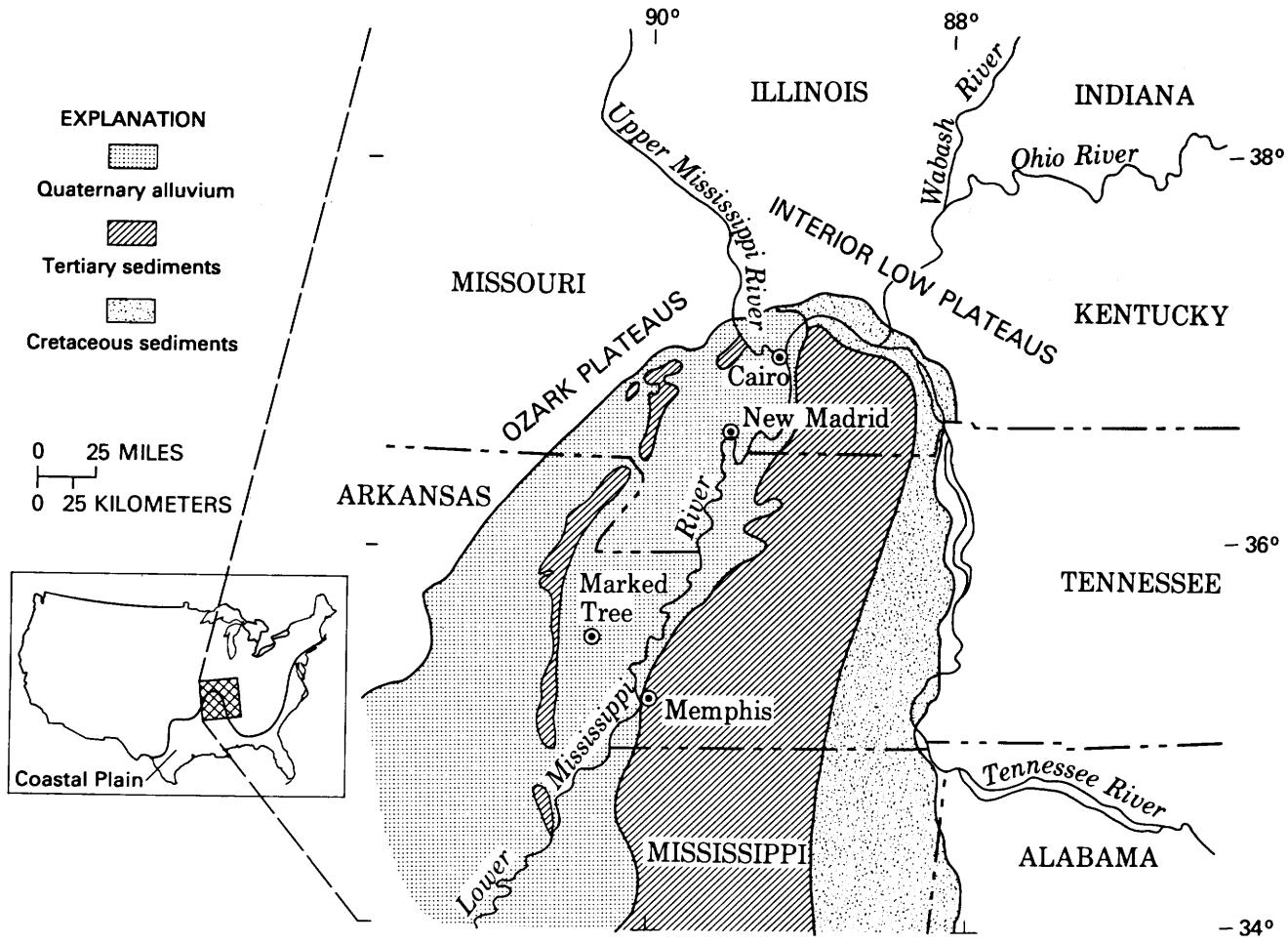

Figure 1. Map of the northern Mississippi embayment of the Gulf Coastal Plain showing the major physiographic features of that area, the distribution of Quaternary alluvium, and Tertiary and Cretaceous sediments.

responsible for much of the total damage. In a reasonably analogous situation, the 1964 Alaska earthquake, liquefaction-induced ground failure caused more than half the economic losses (*Mosaic*, 1979).

Given the possibility of such consequences, exactly where and under what circumstances can liquefaction-induced ground failure be anticipated? Liquefaction generally takes place only in unconsolidated sands or silts, but not all sands or silts have even approximately the same material properties and thus the same liquefaction susceptibility. Important factors other than material properties are earthquake magnitude and ground response characteristics. This paper will present information for evaluating the regional liquefaction potential of different materials in the central Mississippi Valley for different-strength earthquakes. To that end, this paper is organized as follows: (1) a brief review of factors that cause liquefaction and liquefaction-induced ground failure, (2) a description of the historical earthquakes in the central Mississippi Valley, (3) an examination and discussion of two methods that can be used to evaluate liquefaction potential, and (4) a presentation of sediment properties for the geographic area (basically, the alluvial area of fig. 1) where there is a moderate to high probability of liquefaction, given a recurrence of 1811–12-strength earthquakes. This development permits a regional assessment of the liquefaction potential for any earthquake strength.

Because this paper is meant to be understood by geologists, seismologists, and engineers, some replication of common knowledge within each profession is necessary. Where words have different meanings within the different professions (for example, "soil"), it is the commonly accepted engineering interpretation that is intended. Important terms are defined in the text.

Terminology for the relative density of sand strata conforms to usage in table 1. Different earthquake magnitude scales are used in the text. Equivalent values for the different scales are given in table 2.

OVERVIEW OF LIQUEFACTION

Liquefaction is defined as "the transformation of a granular material from a solid state into a liquefied state as

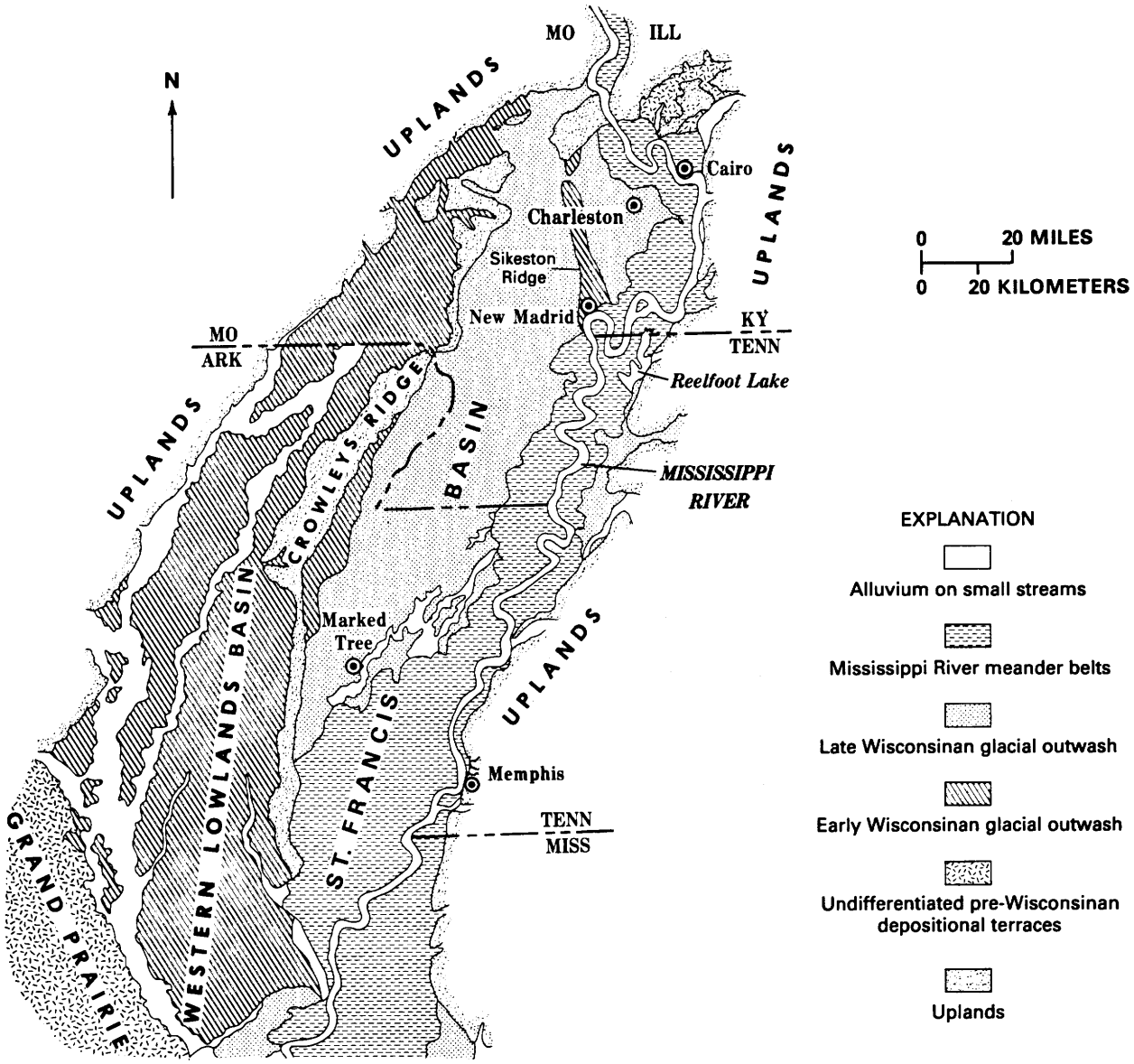

Figure 2. Late Quaternary alluvial deposits in the St. Francis and Western Lowlands Basins (from Saucier, 1974).

a consequence of increased pore water pressures" (Youd, 1973). In the liquefied state, the material basically behaves as a fluid mass.

Conditions for Liquefaction

The application of cyclic shear stresses induced by earthquake ground motions causes a buildup of pore-water pressure in saturated cohesionless soils (Seed, 1979). These stresses are due primarily to the upward propagation of shear waves. A soil element on level ground undergoes loading conditions as depicted in figure 3, the shear stress applications being somewhat random but nonetheless cyclic. Because of this shearing, cohesionless soils that are sufficiently loose would become more compact if pore-water drainage were to occur. Because drainage is usually impeded during the short span of an earthquake, pore-water pressure increases and intergranular stress decreases. If the application of cyclic shear stresses continues, the pore pressure of sands that are packed loosely enough can approach the initial static confining pressure, even though the shear strains are still small. Further cyclic shearing can cause the pore pressure to increase suddenly to the initial confining pressure and thus lead to large shear straining and also flowage.

Although more densely packed cohesionless materials (such as sands having medium or moderate relative density) are not nearly as susceptible to large shear straining as looser materials, they may still develop a residual pore

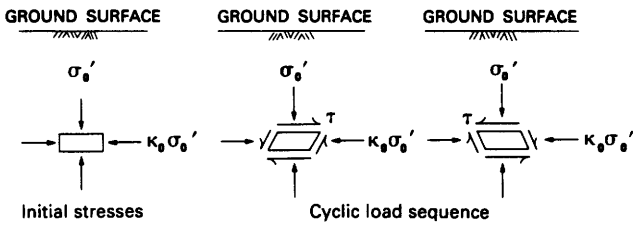

Figure 3. Idealized field loading conditions (from Seed and Idriss, 1971). τ, earthquake-induced horizontal shear stress; σ_0', initial vertical effective overburden stress; K_0, ratio of intial lateral to vertical effective stress.

pressure equal to the confining pressure. After the cyclic stress applications stop, this residual pore pressure generally causes an upward flow of water. It is likely that the upward flow of water to the ground surface from an underlying layer having a high pore-water pressure is the major mechanism for carrying sand to the ground surface and causing "sand blows" (Housner, 1958) or "sand boils" (Seed, 1979). (Sand blows and sand boils are terms often used for the same phenomenon. In this paper, sand blows are restricted to earthquake-induced liquefaction features.)

Liquefaction during earthquake shaking can originate in a zone as shallow as 2 m below the ground surface (Obermeier and others, 1986) to depths much greater than 20 m (Seed, 1979). Generally, if the water table is near the ground surface (say, within a few meters), the probability of liquefaction is significantly increased. However, no simple guidelines are available regarding depth of water table and depth of liquefiable deposits. Figure 4 illustrates that the zone of liquefaction during shaking depends on the relationship between the cyclic shear stresses generated by the earthquake and the stress required to initiate liquefaction in the soil.

Seismological factors of prime importance that control liquefaction during shaking include the amplitude of the cyclic shear stresses and the number of applications of the shear stresses (Seed, 1979). These factors in turn are related to field conditions of shaking amplitude (that is, peak acceleration) and earthquake magnitude. Analytical engineering methods for evaluating variable and irregular cyclic stress applications typical of real earthquakes are well developed and yield results that are quite acceptable for engineering analysis (Seed and others, 1983), providing that shaking amplitude-time records can be predicted with reasonable accuracy.

Table 1. Relative density of sands according to results of Standard Penetration Test blow counts

[From Terzaghi and Peck, 1967]

No. of blows (N)	Relative density
0–4	Very loose
4–10	Loose
10–30	Medium or moderate
30–50	Dense
>50	Very dense

Materials Prone to Liquefaction

Grain-to-grain bonds and the relative density of granular materials are the principal physical controls on liquefaction susceptibility. As granular materials age, grain-to-grain bonds apparently develop and thereby increase resistance to liquefaction; the liquefaction resistance of granular materials having high relative densities is much higher than that of loosely packed granular materials. Very young deposits, less than 500 years in age, are generally much more susceptible to liquefaction than older Holocene-age deposits for a fixed relative density (Youd and Perkins, 1978). As a practical example in the New Madrid region, deposits on modern flood plains generally are more susceptible than slightly older deposits on terraces at slightly higher elevations, even if the ground-water table is at the same depth on the flood plain and terrace (Obermeier and Wingard, 1985).

In areas strongly shaken by the 1811–12 earthquakes, the most common materials susceptible to widespread liquefaction are very loose to medium dense, clean, medium-grained sands that occupy lowland areas; also susceptible are many deposits of gravelly sands and silty and very fine grained sands. Hundreds of rivers and creeks adjoining terraces and flood plains have high water tables and rather loose sands.

Clean silts containing very small amounts of clay and having low cohesion are also susceptible to liquefaction, although not to the extent that many of the clean sands are. Thick, moderately soft, clean silts, deposited as loess, are

Table 2. Earthquake magnitude scales

[This table shows equivalent earthquakes for the central Mississippi Valley. Data are from Nuttli and Herrmann (1982)]

Richter local magnitude (M_L)	Body-wave magnitude (m_b)	Surface-wave magnitude (M_S)
5.0	5.0	4.4
5.2	5.2	4.8
5.4	5.4	5.2
5.6	5.6	5.6
5.8	5.8	6.0
6.0	6.0	6.4
6.2	6.2	6.8
6.4	6.4	7.2
6.6	6.6	7.6
6.8	6.8	8.0
7.0	7.0	8.4
7.2	7.2	8.7

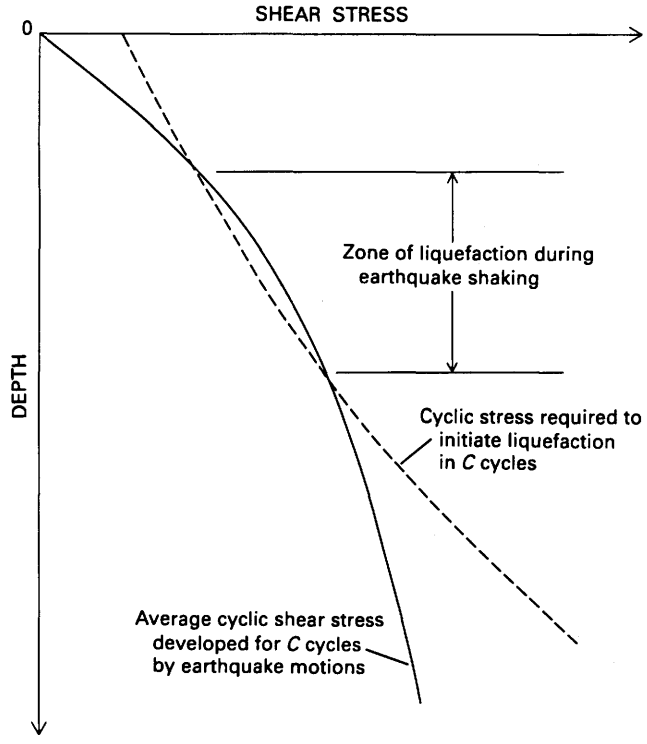

Figure 4. Zone of liquefaction during earthquake shaking (from Seed and Idriss, 1971). *C*, number of cycles.

commonplace in many upland areas near major streams that carried meltwaters from glaciers. Alluvial lowlands adjacent to these loess-covered uplands often have a rather thick veneer of very soft silt, which was originally laid down as loess but was later eroded and redeposited in the lowlands.

Some of the silts in the glacial meltwaters were carried into large lakes and deposited on the lake bottoms. Thick glacial lake deposits of large areal extent are located north and northeast of Cairo. Many of these old lakes have high ground-water tables, and the silts are so clean and soft that they are susceptible to liquefaction. Beneath the silts in these old lake beds are very loose sands at many places.

Clay-bearing soils that may also liquefy appear to be those in which less than 15 percent of the particles are finer than 0.005 mm, the Atterberg liquid limit is less than 35,[1] and the water content[1] is nearly equal to or greater than the liquid limit (Seed and others, 1983). Almost without exception, the only soils exhibiting these properties in the central Mississippi Valley are the silt-rich soils that occupy alluvial lowlands (discussed above) and possibly very young sediments in modern flood plains and in very wet swampy areas.

[1]The liquid limit is the water content at which a remolded sample has a soft consistency; at the liquid limit, the sample is on the semisolid-liquid boundary. Liquid limit is measured in a standardized test described in any elementary soil mechanics text. Water content is the ratio of the weight of water to the weight of dry soil, expressed as a percentage.

It is also possible that clay-rich sediments that are very young (no older than a few tens or hundreds of years) and extremely soft (so soft that the sediments are mud or an ooze) are susceptible to liquefaction. Such weak clay-rich sediments are generally found only adjacent to modern streams.

Consequences of Liquefaction

Liquefaction can lead to three basic types of ground failure (Seed, 1968): flow landslides, landslides having limited movement (lateral spreads), and quick-condition failures. In addition, ejection of soil by sand blows and differential loosening and densifying of soil can cause differential settling of the ground surface. For sands, Youd (1978) has suggested that the type of ground failure induced by liquefaction is related to the ground surface slope, as table 3 shows.

Thickness and setting (for example, the depth or lateral continuity of the sand deposit) also need to be considered in determining the probable mode of ground failure. A thin, loose sand layer at a depth of 10 m in an otherwise nonliquefiable clay deposit is not likely to cause a bearing capacity failure, regardless of the ground surface slope. However, this condition might lead to a translational landslide on steep slopes or magnify ground surface movement due to lateral spreading in flat areas (Anderson and others, 1982).

Flow Landslides

On slopes steeper than 5 percent, large soil masses can move as viscous fluids or blocks of intact materials riding on liquefied flows. Liquefaction in sands and silts can lead to flows that travel hundreds of meters (see, for example, Youd and Hoose, 1978, figs. 20–22). Some of the most destructive flows ever recorded originated in loess on hill slopes in Russia (Keefer, 1984).

Lateral-Spread Landslides

Limited flow can take place on slopes between 0.5 and 5 percent, underlain by sands or silts that are too dense to flow freely. Where loose sands occur on slope inclina-

Table 3. Ground slope and expected failure mode of coarse-grained deposits liquefied during earthquakes
[After Youd, 1978]

Ground surface slope (percent)	Failure mode
<0.5	Bearing capacity and ground oscilliation.
0.5–5	Lateral-spread landslides
>5	Flow landslide

tions of as little as 0.5 percent, horizontal displacements can still be many meters and leave large open cracks at the surface (Youd, 1978). Generally, lateral spreads develop in alluvial lowlands along streams. Lateral spreads are generally longest parallel to the streams. Lengths along streams of 150 to 300 m are not unusual (see, for example, Fuller, 1912). Rather large lateral spreads can also develop wherever lateral resistance to movement is reduced by removal of only a few meters of soil. Small scarps and manmade ditches are likely locations. Lateral spreads are commonplace in alluvium as a result of moderate to strong earthquakes.

Quick-Condition Failures

Seepage forces caused by upward-percolating pore water can drastically reduce the shear strength of granular materials for a period of minutes to days after earthquake shaking. If the strength is reduced to the point of instability, this state is known as a "quick condition."

Quick-condition failures are generally found only in thick sand deposits that extend from below the water table to the ground surface. Loss of bearing capacity is a common type of quick-condition failure. During the 1964 Niigata earthquake in Japan, high-rise apartment buildings had quick-condition bearing-capacity failures and rotated so much that people could walk on previously vertical exteriors; embankments also subsided into the weakened sands. The buoyant rise of buried tanks, empty swimming pools, and water treatment tanks is another common result.

Differential Settlements

Wherever seepage forces carry sand and water to the surface, buildings can be undermined. Vertical displacement of the ground surface by densification of a liquefied soil layer can cause differential settling of buildings. Although differntial settling is probably not often totally destructive of buildings, it can distort and damage structures.

Engineering Evaluation of Liquefaction Potential

Methods developed recently to determine material properties include the electric-cone penetration test, the cross-hole seismic velocity test, and the pressuremeter test (Youd and Bennett, 1983). These test methods, which are still somewhat experimental, have yielded so few data in the central Mississippi Valley that it is not reasonable to consider their use for regional evaluation of liquefaction potential. Laboratory dynamic test data on natural soils are virtually nonexistent for the central Mississippi Valley, and, for a regional evaluation of liquefaction potential, developing an adequate data base by means of dynamic laboratory testing would be prohibitively expensive. The only method for which there are abundant data is the Standard Penetration Test (SPT).

In the field, evaluating the properties of sand deposits is most commonly done, at least for preliminary or regional analysis, by testing the soil in place with the SPT blow count method (American Society for Testing and Materials, 1978). A sampling tube is driven into the ground by dropping a 140-lb (63.5-kg) weight from a height of 30 in (176.2 cm). The penetration resistance is measured by the number of blows required to drive the sampler 1 ft (30.5 cm). The SPT blow counts (N values) are then used in conjunction with anticipated earthquake-induced shear stresses and number of repetitions of the shear stress (which is related to earthquake magnitude) to determine if liquefaction can take place. Figure 5 shows boundary curves (Seed and others, 1983) that define where liquefaction is likely to occur for earthquakes of different magnitudes. The curves apply to clean sands containing almost no silt, on level ground. (Figure 5 can be modified for use with silty sands and clean silts that plot below the A line on the Unified System plasticity chart (Seed and others, 1983, p. 479) by adding 7.5 to the N_1 value.) For a given earthquake magnitude, data points below the curve have a high probability of not liquefying, and data points above the curve have a high probability of liquefying enough to cause sand blows (and landslides and other liquefaction-related ground failure). The curves were developed from field and theoretical studies of earthquake-induced liquefaction at many sites around the world.

The field cyclic stress ratio in figure 5 is the ratio, on an element in the sand layer, of the average earthquake-induced horizontal cyclic shear stress ($\tau_{h\ avg}$) to the vertical effective stress (σ_0') before the cyclic stresses were applied. The field cyclic stress ratio due to earthquake shaking, developed in the field, is computed from the following equation (Seed and others, 1983):

$$\frac{\tau_{h\ avg}}{\sigma_0'} = \frac{0.65(A_{max} \cdot \sigma_0 \cdot r_g)}{g \cdot \sigma_0'}$$

where A_{max} is the peak horizontal acceleration at the ground surface, σ_0 is the total overburden stress on the sand under consideration, σ_0' is the initial effective overburden stress (total stress minus pore-water pressure) on the sand layer under consideration, r_g is the stress reduction factor ranging from a value of 1 at the ground surface to a value near 0.9 at a depth of about 10 m, and g is the acceleration of gravity.

For one of the most common field conditions on alluvium in the New Madrid earthquake region, where the water table is about 2 m below the ground surface and the weakest sands are at a depth of 4 to 5 m, the field cyclic stress ratio is almost exactly equal to the peak horizontal acceleration; that is, if the peak horizontal acceleration is 0.20 g, the cyclic stress ratio is essentially 0.20. In figure 5,

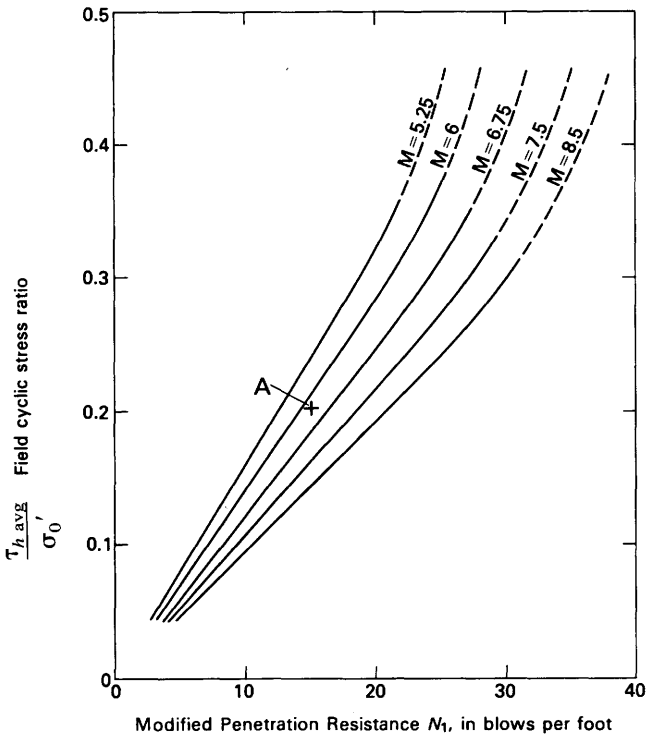

Figure 5. Evaluation on level ground of liquefaction potential of clean sand deposits (average diameter >0.25 mm) for different magnitude earthquakes (from Seed and others, 1983). A is a data point indicating probable liquefaction for M=6.75 (discussed in text). M is earthquake magnitude (Richter magnitude M_L or surface-wave magnitude M_S, whichever is larger).

the modified penetration resistance N_1 is the SPT blow count value measured in the field multiplied by a correction factor that accounts for the influence of field stress conditions on the measured blow count; for the field conditions just given, the multiplication factor is 1.4 (see Seed and others, 1983).

To illustrate use of the curves, assume that the peak horizontal acceleration at the ground surface is 0.20 *g* for an earthquake magnitude (M) of 6.75 and that the SPT blow count in clean sand is 11 (corrected to $N_1 = 15.4$) on a nearly level terrace for the depth and water table conditions described above. This situation is shown as point A in figure 5; liquefaction and production of sand blows would be very probable.

The accelerations required for liquefaction according to figure 5 are an approximate lower bound. Figure 6 shows the curve for M = 7.5 and field data from many earthquakes around the world. The solid circles in figure 6 represent data taken from sites where there was evidence of liquefaction-induced ground failure, such as sand blows. Although no evidence for liquefaction was observed at some sites (open circles), liquefaction still may still have occurred at depth and not been observed because the field setting was not conducive to production of sand blows. To illustrate, an especially thick, fine-grained cap above liquefied sands apparently prevented sand blows from venting to the ground surface at many places in the St. Francis Basin during the 1811-12 earthquakes (Saucier, 1977), yet many dikes and sills of liquefied sediment penetrated the cap (S.F. Obermeier, unpublished data, 1979). As another example, especially coarse and permeable deposits above the zone lique-

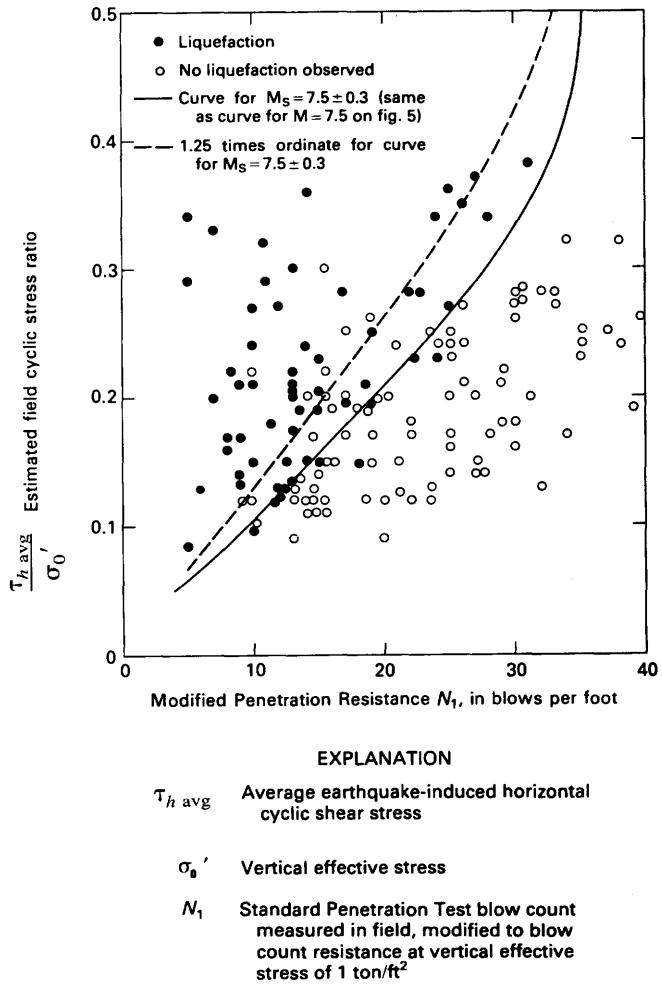

Figure 6. Correlation on level ground between field liquefaction behavior of sand deposits (average diameter >0.25 mm) and modified penetration resistance for surface-wave magnitude M_S=7.5 ±0.3 (from Seed and Idriss, 1982).

fied during shaking appear to have dissipated pore pressures so fast in many places that sand blows did not develop (Obermeier, in press). The data in figure 6 are from many types of field settings, scattered around the world, and it is not surprising that expressions of liquefaction-related features were not observed, even though liquefaction may have occurred. In summary, the solid line in figure 6 is probably quite a good bound for estimating accelerations, provided that attention is given to the field setting; in addition, it is extremely likely that there would be liquefaction at accelerations 25 percent higher than those shown by the solid line- bound (see fig. 6).

Figure 5 is strictly applicable for level or nearly level ground only (that is, for slopes less than about 5 percent). On steeper slopes, higher accelerations may be required to cause liquefaction, and more sophisticated methods must be used to determine if liquefaction can develop. Still, using figure 5 helps assess the possibility of problems on the slopes; if ground failure is indicated by figure 5, the potential for problems warrants further investigation.

The procedure sketched above, known as the Simplified Procedure of Seed and Idriss, indicates only where liquefaction is probable. Damaging ground failure may or may not result from an occurrence of liquefaction. In general, liquefied loose sands are much more likely to flow, move large distances, and cause more damage than liquefied medium dense sands are; more rigorous methods are necessary for evaluating the complete scenario.

For clay-bearing soils that plot above the A line on the Unified Classification System plasticity chart (Seed and others, 1983, p. 479), there are no charts analogous to figure 5. Laboratory test methods must be used at the present time to appraise their behavior in any detail. However, it is certain that serious liquefaction can take place in these materials only if they are very soft. The softness of silts and clays can also be crudely estimated by the SPT method. Only very weak, clay-bearing soils that have index and physical properties (natural water content, liquid limit, percentage of clay) in the range discussed previously are candidates for liquefaction.

LIQUEFACTION AND HISTORICAL EARTHQUAKES

Historical earthquakes in the central Mississippi Valley can be used to establish relations between liquefaction, earthquake magnitudes, accelerations, and Modified Mercalli (MM) intensities. Liquefaction effects of the 1811–12 earthquakes are reviewed first; accounts of more recent earthquakes having body-wave magnitudes (m_b) greater than 5.3 follow.

1811–12 Earthquakes

It is well known (Fuller, 1912) that great numbers of liquefaction-induced ground failures (hereafter referred to as "liquefaction" or "liquefaction features") took place many tens of kilometers from the probable epicenters of the 1811–12 earthquakes and locally were as far away as 400 km (Fuller, 1912, p. 19). Accounts of areas where the farthest liquefaction effects were fairly common typically describe disappearing islands in rivers, sand blows near streams, and lateral spreads along stream banks. Most, if not all, of these farthest liquefaction features were probably in very young alluvial sediments.

The late Quaternary and Holocene sediments in the central Mississippi Valley are from a variety of flow regimes and, in addition, range in thickness from a featheredge to many tens of meters. There are large differences in liquefaction susceptibility and physical properties in these sediments (Obermeier and Wingard, 1985) because of differences in their ages and modes of deposition. The liquefaction susceptibility of deposits on modern flood plains commonly is much higher than that of Wisconsinan-age sediment. This large variation in physical properties and thicknesses also causes wide variations in ground response characteristics. Thus, using the regional pattern of liquefaction features to understand earthquake characteristics (such as epicenter locations and accelerations) would be extremely difficult in a highly variable geologic setting, such as one in which all sediment ages and depositional modes are present. However, the uniform thickness and relatively similar liquefaction susceptibility and physical properties of late Quaternary alluvium, which is widespread throughout the St. Francis and Western Lowlands Basins, present an almost ideal setting for a study of the 1811–12 earthquakes.

Alluvium in St. Francis and Western Lowlands Basins

Figure 2 shows alluvial deposits in the St. Francis and Western Lowlands Basins. Almost all the deposits shown in the eastern two-thirds of the figure are late Quaternary in age; only locally, generally on modern flood plains, are there significant deposits of much younger alluvium. Total thickness of alluvium is typically between 30 and 50 m throughout the St. Francis Basin (Saucier, 1964), and the thickness is only slightly less in the Western Lowlands Basin (Smith and Saucier, 1971).

Alluvium in the Western Lowlands Basin and between the towns of Cairo and Marked Tree is mostly braided stream terraces of glacial outwash. These terraces are typically a layered sequence of "topstratum" over "bottomstratum" (Saucier, 1964). The topstratum is generally

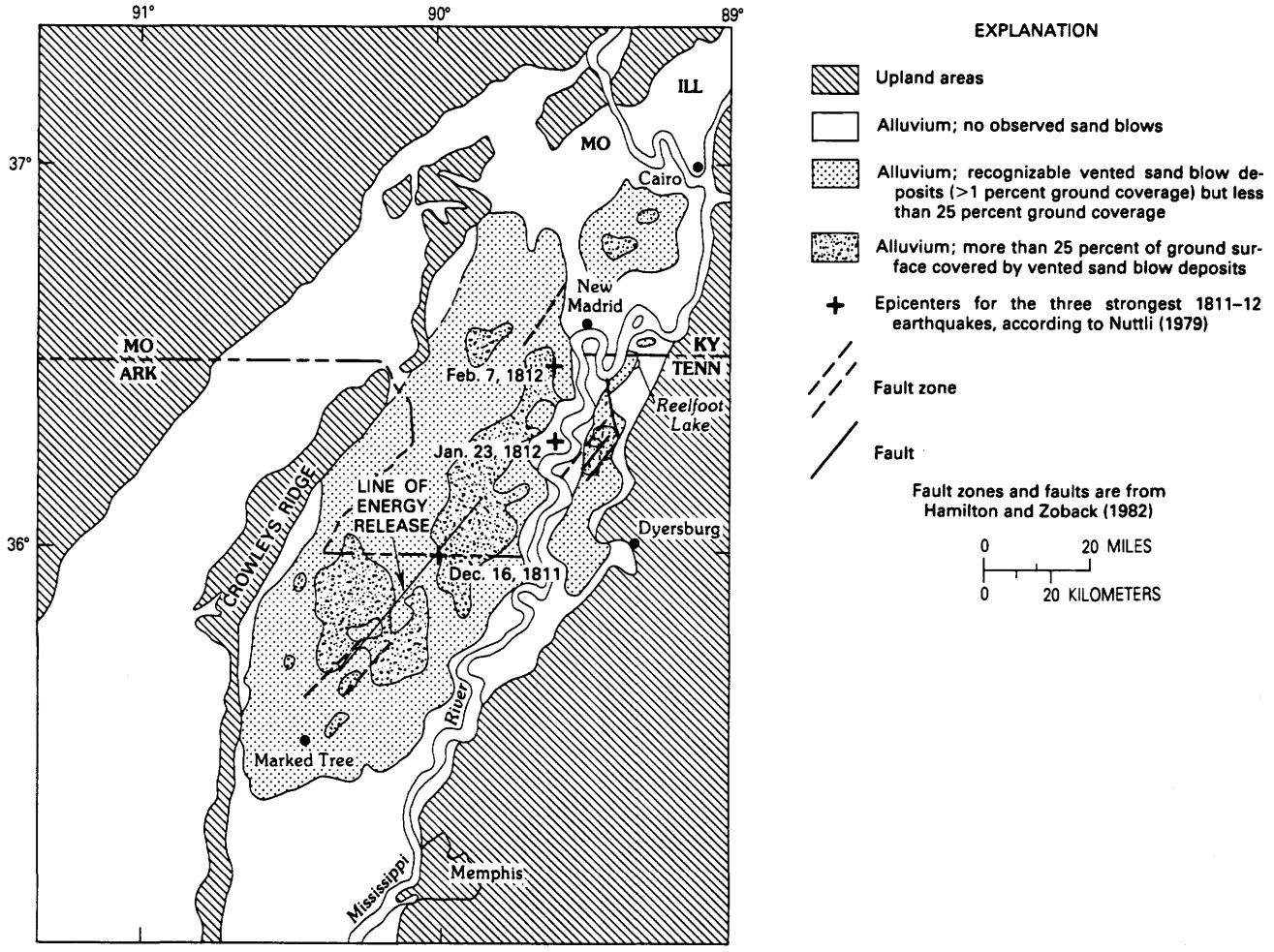

Figure 7. Distribution of vented sand blow deposits on alluvium excluding modern flood plains (Obermeier, in press). Sand blows were presumably formed by the 1811–12 earthquakes. Also shown are the energy release center line for the December 16, 1811, earthquake and fault zones and faults.

a 2- to 6-m-thick overbank deposit, composed primarily of thick to thin strata that are very rich in clay and highly plastic. The clay strata are interbedded with less common strata of silt and very fine sand. The contact of the topstratum on the bottomstratum is typically gradational over a meter. The bottomstratum is a very clean, moderately dense sand, which is generally fine to medium grained near the top and grades downward to a coarse sand that has gravel at its base.

Meander belt deposits of the Mississippi River generally have thick strata of clean, fine- to medium-grained sand, silty fine sand, and clay within the uppermost 10 to 15 m. Beneath that are clean sands that coarsen with depth and are representative of the bottomstratum. A clay-rich cap of overbank deposits covers these meander belt deposits at many places, especially in swales and sloughs. The thickness of the clay-rich cap is generally less than 10 m. Within these meander belts, there are usually many localities (within a few hundred meters of one another) where the clay cap is only a few meters thick, and clean sand underlies the cap.

Sand Blow Deposits in St. Francis Basin

Figure 7 shows the distribution and concentration (that is, proportion of area covered) of sand blow deposits in the St. Francis Basin, excluding alluvium of modern flood plains. Figure 7 is based on an investigation by the author, who used 1938–40 vintage aerial photographs and more recent ones (scale about 1:20,000) in conjunction with field verification. Field and aerial photographic studies represented in figure 7 were restricted to the St. Francis Basin and the eastern one-third to one-half of the Western Lowlands Basin (that is, the area of alluvium west of Crowleys Ridge). No sand blow deposits were found in the Western Lowlands Basin.

Much of the field and aerial photographic study was directed at locating the margin of liquefaction effects,

which was empirically defined as the outer limit where at least 1 percent of the ground surface is covered by sand blow deposits (smaller percentages are difficult to determine from aerial photographs). In that way, the location of the epicenter (more accurately, the "energy release center"[2]) can be estimated for the December 16, 1811, earthquake, and earthquake accelerations can be estimated away from near-field earthquake effects by using the relations in shown figure 5.

Energy Release Center

On the basis of regional earthquake intensity studies, Nuttli (1979) estimated that the three largest 1811–12 earthquakes had the epicenter (energy release center) locations shown in figure 7. Although the epicenter locations are very approximate, it is likely that the first strong earthquake, the December 16 event, was located considerably southwest of the other two. Thus, it seems reasonable to associate the southernmost third of the sand blow deposits with the December 16 event. (The three largest earthquakes were of approximately the same strength.) Estimated epicenters for the other two large events are so close to one another that there is less credibility in using the distribution of sand blow deposits to locate their energy release centers.

A cursory examination of figure 7 suggests that the energy release center for the December 16 earthquake lies somewhere along a line centrally located with respect to the boundary of sand blow deposits, roughly in the southern third of these deposits. In addition, the line trends southwest-northeast and has a southern terminus north of Marked Tree. This location is based on the premise that the alluvium in the region, excluding very young alluvium of the modern flood plains, has about the same physical setting and engineering properties throughout the area and thus the same liquefaction susceptibility. To examine this premise, the author investigated alluvium in the St. Francis and Western Lowlands Basins by compiling some 400 boring logs. Most of the data were collected from files of the U.S. Army Corps of Engineers, Memphis District. About 250 of the logs had SPT data to depths of about 12 to 15 m. The boring locations were scattered throughout the area, but most were near levees of large drainage ditches. Data from very young alluvium and alluvium along most small streams (that is, modern flood plain deposits) were excluded.

The data are separated in table 4 according to the following geographic-geologic settings: braided stream terraces in the Western Lowlands Basin, the southern half of braided stream terraces in the St. Francis Basin, and Mississippi River meander belt deposits. The southern half of braided stream terraces in the St. Francis Basin is further subdivided into four large areas. Strata of silty, very fine grained sand and of very fine sand are much more common in meander belt deposits than they are in braided stream terrace deposits, which generally have coarser sands. This textural difference required a correction to the SPT blow count (the method of Tokimatsu and Yoshimi (1981) was used) to account for the influence of grain size on liquefaction potential. There are no substantive differences in SPT blow counts or sand textures in braided stream deposits throughout the southern part of the St. Francis Basin.

Table 4. Modified penetration resistance values (N_1) in selected settings in the Western Lowlands and St. Francis Basins

Geologic-geographic setting	Median N_1[1]	Lower quartile N_1[1]	No. of borings
Braided stream terrace deposits, Western Lowlands Basin	22–23	15	17
Braided stream terrace deposits, southern half, St. Francis Basin	26	15–20	105
Meander belt deposits of Mississippi River	25	12–18	48

[1] N_1 is the modified penetration resistance, as discussed by Seed and others (1983). N_1 values are for a depth range of 3 to 10 m.

Table 4 shows "modified penetration resistance" (N_1) values (N_1 is defined in fig. 5), which is the field SPT blow count modified to account for the influence of overburden pressure and water table location. The N_1 values are for a depth range of 3 to 10 m, which is the range generally most susceptible to liquefaction in these basins (at greater depths, N_1 values are generally higher (Obermeier, in press)). Median and lower quartile values (that is, the 50- and 25-percent values) are given because they are thought by the author to realistically bracket the percentage of a sand body in this depth range that must be liquefied to form a minor regional development of liquefaction, as evidenced by the ground being covered by at least 1 percent of vented sand. Requiring that half the volume of sand liquefy seems an unrealistically high requirement, because liquefaction of a single layer of sand 2 to 4 m thick (having N_1 values of up to 13-15) can be enough to cause liquefaction-induced damage to structures (Ishihara, 1985) at a peak horizontal acceleration of about 0.2 to 0.25 g and a surface-wave magnitude of about 7.6 to 7.8 (magnitudes considerably lower than those of the three strongest 1811–12 New Madrid earthquakes). Liquefaction that is sufficient to cause damage to structures is probably more severe than liquefaction that is adequate simply to induce minor regional development of sand blows. For a minor regional development of sand blow deposits, however, there must also be

[2] The epicenter is the point on the Earth's surface directly above the earthquake focus (the focus is the point at which strain energy is first converted to elastic wave energy). Thus, the epicenter may or may not be coincident with the point or zone of maximum energy release (that is, the "energy release center").

some significant degree of liquefaction, although the lower cutoff is very uncertain and must depend on factors other than N_1 (for example, important factors in the 1811–12 earthquake were topstratum thickness and the grain size of the liquefied stratum (Obermeier, in press)). The requirement that somewhere between 25 and 50 percent of the sand in the depth range 3 to 10 m must have liquefied (that is, 2–3.5 m must have liquefied) seems consistent with boundary curves proposed by Ishihara (1985, fig. 88) showing relations between the thickness of the nonliquefiable cap and that of liquefied sand bed for different accelerations.

Regardless of whether the median or lower quartile or a lower value is more appropriate, table 4 shows that, in the St. Francis Basin, N_1 values are about the same in braided stream terrace deposits and in Mississippi River meander belt deposits, and N_1 values for both types of St. Francis Basin alluvium tend to be slightly higher than those for Western Lowland braided stream terrace alluvium. The topstratum is so thin at many places (less than 3–4 m) in both the Western Lowlands and the St. Francis Basins that an excessive topstratum thickness could not have been a major factor in defining the outer bound of sand blow deposits, at least regionally (Obermeier, in press). Thus, the energy release center line (hereafter also referred to as the energy release line) for the earthquake of December 16, 1811, should lie approximately central to the outer limits of sand blow deposits. This central location establishes the southernmost possible terminus and the orientation of the energy release line shown in figure 7. The length of the energy release line (about 60 km) is based on Nuttli's (1983) estimate of the length of rupture.

Other data strongly suggest that the fault that caused the December 16 earthquake was strike-slip and was parallel to and very close to the energy release line in figure 7; as examples, modern seismic activity (Stauder, 1982) takes place near the energy release line, and the stress field in lithified rocks is oriented east-west (Hamilton and Zoback, 1982). In addition, the overall style of surface deformation near Reelfoot Lake is consistent with a fault zone extending from the vicinity of the lake toward Marked Tree (Russ, 1982). Data on modern microearthquakes suggest that the rupture depth was between 3 and 13 km (Nicholson and others, 1984).

Accelerations in Alluvium

Sites generally best suited for back-calculating earthquake accelerations on the basis of liquefaction are outer margin locations of sand blow deposits at sites of marginal liquefaction, where liquefaction causes only minor changes in preearthquake and postearthquake SPT blow counts. This outer margin is less than 40 km from the axis and from the southern terminus of the energy release line. No SPT data were available along the margin of sand blows in figure 7, so N_1 values are used in the region of liquefaction.

N_1 values of 20 or less comprise at least 25 percent of the SPT data points in the depth range 3 to 10 m (table 4) in the region of sand blows produced by the December 16 earthquake, shown in figure 7. Using this N_1 value of 20 as appropriate at the border of sand blows yields a threshold acceleration of slightly more than 0.20 g required to generate liquefaction, assuming that the N_1 values were not greatly changed by the earthquake. This assumption seems reasonable in view of the facts that (1) SPT blow counts and the geologic settings are about the same in both the Western Lowlands and the St. Francis Basins and (2) the Western Lowlands Basin did not experience significant liquefaction during the 1811–12 earthquakes. In summary, it is very probable that, 40 to 45 km from the energy release line, the peak horizontal accelerations at the ground surface were less than 0.20 g.

Accelerations in Bedrock

The lack of strong-motion ground response data for the New Madrid earthquake region makes it necessary to relate the acceleration in alluvium to bedrock motion by empirical relations developed elsewhere and by semiquantitative calculations. Seed and Idriss (1982, p. 37) have shown that, on average, at 0.20 g, the peak acceleration in rock is nearly the same or only slightly higher than that in overlying stiff or thick cohesionless soil. These cohesionless soils presumably range from loosely to densely packed. For strong earthquakes, Ishihara (1985, p. 353) stated that "It may as well be argued that the ratio of acceleration on the soil deposit to that on the rock outcrop causing liquefaction in their area is approximately in the range 0.65 to 0.9 with an average of about 0.8." Sharma and Kovacs (1980), in a microzonation study of the Memphis area using the computer program SHAKE and synthetic seismograms, found that the moderately thick (about 30–40 m), medium densely packed sands of the area probably have peak accelerations that are about the same as those in the underlying bedrock for strong earthquakes in the New Madrid fault zone (their New Madrid fault zone includes the energy release center line in fig. 7); their data show that the peak accelerations in these sands should range from about equal to but not more than about 20 percent higher than those in the underlying bedrock.[3] All the accelerations back-calculated from SPT-liquefaction relations in the preceding section are from sites where sand is about 30 to 50 m thick. Thus, it is likely that, at these sites, the peak accelerations at the ground surface were about the same as or else only slightly (±20 percent) higher or lower than those in the bedrock beneath.

[3]Sharma and Kovacs made acceleration amplification calculations both for a basal stratum of sand and of gravel. The author believes that the results for sand are most applicable to the southern half of the St. Francis Basin because of the preponderance of sand.

Table 5. Locations, intensities, and liquefactions of central Mississippi Valley historical earthquakes having body-wave magnitudes greater than or equal to 5.3, exclusive of 1811–12 earthquakes

Location[1]	Date	Modified Mercalli intensity[2]	Body-wave magnitude[1]	Liquefaction[2]
Mississippi embayment:				
lat 35.2° N., long 90.5° W.	1–4–1843	VIII (minimum)	6.0	None reported
lat 36.5° N., long 89.5° W.	8–17–1865	VII	5.3	None reported
lat 37.0° N., long 89.4° W.	10–31–1895	VIII	6.2	Commonplace
lat 36.9° N., long 87.3° W.	11–4–1903	VII	5.3	None reported
Wabash Valley:				
lat 39.0° N., long 87.7° W.	9–27–1909	VII	5.3	None reported
Mississippi embayment:				
lat 5.5° N., long 90.3° W.	10–28–1923	VII	5.3	None reported
lat 36.5° N., long 89.0° W.	5–7–1927	VII	5.3	None reported
Wabash Valley:				
lat 38.0° N., long 88.5° W.	11–9–1968	VII	5.5	None reported

[1]Nuttli and Herrmann (1978).
[2]Coffman and von Hake (1973).

Farthest Liquefaction

The farthest lateral spreads or flows were about 175 km from the 1811–12 earthquake epicenters, according to Keefer (1984). O.W. Nuttli (oral communication, 1983) has found historical accounts that mention sand blow activity on the flood plain of the Mississippi River, near St. Louis. Street and Nuttli (1984) reported sand blows and fissures in White County, Illinois, along the Wabash River. These sand blows probably formed in deposits in which N_1 values of 10 or less are common (Obermeier and Wingard, 1985). Both St. Louis and White County are less than 300 km from the general vicinity of the epicenter for the February 7, 1812, earthquake (see fig. 7 for epicenter location).

According to Street and Nuttli (1984), the southernmost limit of the damaged area for the December 16 earthquake was either Island 53 or Island 57 in the Mississippi River. It is possible that liquefaction caused the damage on these islands, which are about 350 km south of the probable epicenter (fig. 7) for the December 16 earthquake.

Other Historical Earthquakes

Table 5 is a compilation of central Mississipi Valley historical earthquakes having body-wave magnitudes equal to or higher than 5.3 and the associated accounts of liquefaction and and MM intensities. Liquefaction was reported only for the October 31, 1895, earthquake (which is also known as the Charleston, Mo., 1895 earthquake). Sand blows occurred at scattered locations over a region about 16 km in diameter, at places north of Charleston, in Charleston, and south and southwest of Charleston (Powell, 1975). The region where sand blows developed is in Late Wisconsinan braided stream (glacial outwash) alluvium (see fig. 2), which is only a little less susceptible to liquefaction than alluvium elsewhere in the Western Lowlands and St. Francis Basins (excluding very young alluvium). Thus, a reasonable threshold for liquefaction is $m_b = 5.5$ to 6.0 for braided stream and meander belt deposits in both basins, excluding deposits on modern flood plains.

Earthquake Intensity and Liquefaction

Table 5 lists no reports of liquefaction for MM VII[4] or lower. Alternately, the MM VIII area of the 1895 Charleston earthquake, for which sand blows were reported, is in an area where the sediments are medium dense and at least moderately difficult to liquefy. It seems incongruous that there are no accounts in table 5 of liquefaction for the 1895 earthquake or any other earthquakes in loose flood plain deposits for MM VII, and yet liquefaction did occur in moderately dense materials for MM VIII. The author thinks it probable that there were sand blows in the flood plain alluvium, especially the very young (less than 500 years old) alluvium for many of the MM VII-producing earthquakes but that sand blows were not reported. Sand boils develop in the flood plain behind both natural and artificial levees along the Mississippi River after many of the largest annual floods, because of the large difference in hydraulic head on opposite sides of the levees. Thus, in 1895, the sand blows in these lowland regions may not have received special attention.

Figure 8 is a map prepared by Nuttli (1981) showing regional intensity data for the December 16, 1811, earthquake. Locations of farthest sand blows (in the Mississippi River flood plain near St. Louis and in the Wabash River

[4]MM intensity values in table 5 are regional values rather than absolute maximum values that are present within a region. At a given site, intensity values are commonly one unit higher or lower than regional values; site MM intensity values are two units higher in exceptional places.

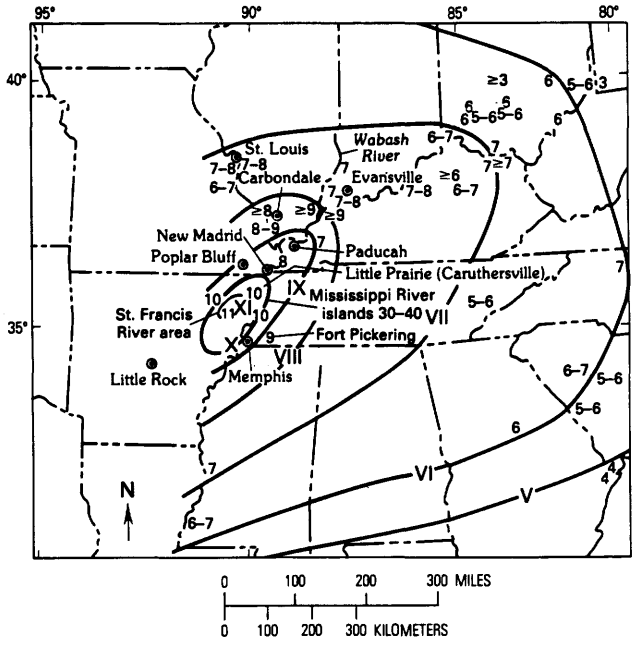

Figure 8. Modified Mercalli intensities for the December 16, 1811, earthquake (from Nuttli, 1981).

valley) are in the zone of MM VII intensity. Thus, it is concluded that a regional MM VII is the liquefaction threshold for the very loose flood plain sands, regardless of earthquake magnitude. This intensity conforms to Keefer's (1984) findings.

SUGGESTED METHODS FOR EVALUATING LIQUEFACTION POTENTIAL

Acceleration, magnitude, intensity, and liquefaction data are examined in this section to develop independent approaches for evaluating liquefaction potential.

Simplified Procedure of Seed and Idriss

The Simplified Procedure of Seed and Idriss requires an acceleration–epicentral distance relationship for various earthquake magnitudes in order to be versatile. Data compiled by Nuttli and Herrmann (1984a) are used in combination with acceleration data at the margin of sand blows (from this paper) to develop acceleration–epicentral distance relations.

Figure 9 is a plot done by Nuttli and Herrmann (1984a) showing the arithmetic average of peak values of horizontal acceleration (average of two components) for stiff soil as a function of epicentral distance and body-wave magnitude for the Central United States. Athough Nuttli and Herrmann did not so state in their text, their epicenter is assumed to be coincident with the point of maximum energy release. The Nuttli-Herrman curves of acceleration–epicentral distance in figure 9 are based on semitheoretical calculations, in combination with measured accelerations on small- to moderate-sized earthquakes in the New Madrid region. The error of estimate for one standard deviation for the Nuttli-Herrmann curves is a factor of 1.74.

The curves in figure 9 are intended to be applicable to stiff soil (Nuttli and Herrmann, 1984a). Stiff soils may (and probably do) amplify bedrock accelerations in the New Madrid earthquake region, as calculations by Sharma and Kovacs (1980) indicate. Bedrock accelerations are amplified a small to moderate amount (that is, by a factor of 1.1–1.4) for small to moderate accelerations for earthquakes of the size (mainly $m_b<5.5$) from which figure 9 was developed. The amount of amplification for unconsolidated materials also varies somewhat as a function of epicentral distance, acceleration level, and layer thickness.

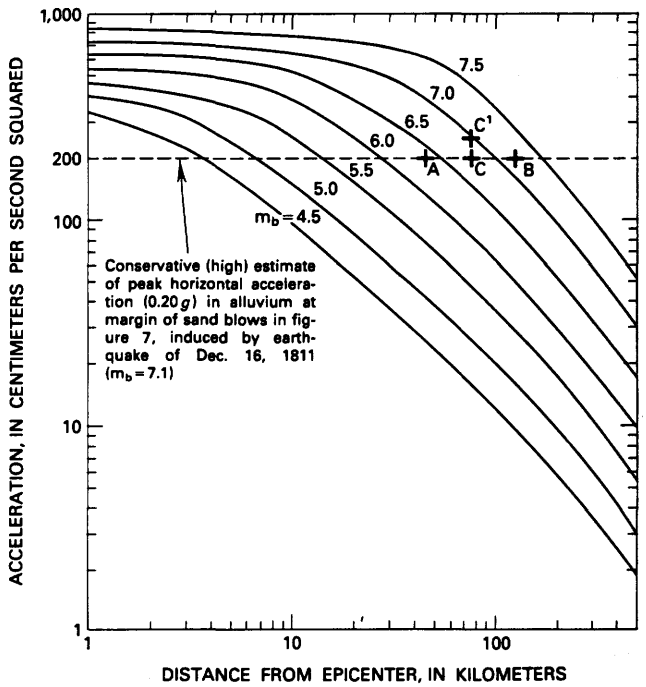

Figure 9. Curves for peak horizontal acceleration on stiff soils (arithmetic average of peak accelerations on the two horizontal components) versus epicentral distance for various body-wave magnitudes (from Nuttli and Herrmann, 1984a), and back-calculated December 16, 1811, accelerations for St. Francis Basin alluvium (this paper). Back-calculated December 16, 1811, accelerations are based on liquefaction data. A, Minimum possible distance (40–45 km) from the epicenter of the December 16, 1811, earthquake to the margin of sand blows; B, maximum possible distance (110 km) from the epicenter of the December 16, 1811, earthquake to the margin of sand blows; C, "most probable" epicentral distance (75–80 km); C^1, maximum peak horizontal acceleration in underlying bedrock that can be reasonably associated with the most probable epicentral distance (75–80 km). Curves are based almost exclusively on modern acceleration data from earthquakes where $m_b<5.5$. Standard deviation of log acceleration values about the $m_b=5.0$ curve is 0.24.

Thus, the basis for extrapolation to large earthquakes used for the Nuttli-Herrmann curves of figure 9 and the relations of the curves to bedrock motions are not clearly known, but, for now, it is assumed that the curves are applicable to bedrock accelerations.

The energy release line shown on figure 7 is centrally located with respect to the boundary of sand blows in the St. Francis Basin; the southern terminus is taken to be the center of a semicircle described by the sand blow boundary (not shown). It now is assumed that the epicenter of the December 16 earthquake was somewhere along the energy release line. Given this constraint, some bounds can be placed on acceleration as a function of distance from the epicenter. The peak horizontal acceleration in bedrock for the December 16 earthquake, previously determined in this report to be near the margin of sand blow deposits, was probably not greater than about 0.20 *g*. The southern end of the energy release line is less than 40 km from the margin of sand blows. Using this distance conservatively yields (for hazard analysis) a peak horizontal acceleration of 0.20 *g* at 40 to 45 km from the epicenter (point A, fig. 9). Point A is probably a slightly conservative (that is, high) estimate of acceleration at this lower bound epicentral distance 40 to 45 km from the epicenter.

The farthest possible northward location of an epicenter is midway between the southern limit of sand blows (south of Marked Tree) and the northern limit (near Cairo). If the epicenter had been farther north, widespread liquefaction would have occurred beyond the limits of sand blows northwest of New Madrid (fig. 7), in the braided stream deposits between Sikeston Ridge and Crowleys Ridge (fig. 2), because braided stream deposits throughout the St. Francis Basin have about the same liquefaction susceptibility and, locally, at many places have about the same ability to produce sand blows. Thus, as a maximum, the peak horizontal acceleration was 0.20 *g* 110 km from the epicenter, which would be located near the northern terminus of the energy release line in figure 7 (point B, fig. 9). This upper bound includes the maximum possible effects of focusing along a strike-slip fault. Point B is the point that the author considers as the absurd upper limit. Almost certainly, the northern limits of sand blows were the result of the February 7, 1812, earthquake, which probably had its epicenter in the general vicinity of New Madrid and Reelfoot Lake (Nuttli, 1979).

A reasonable southern limit for the energy release line (not epicenter) for the December 16 earthquake is somewhere in the center of the southernmost large area where vented sand covers more than 25 percent of the ground surface (fig. 7). Throughout much of this large area, the volume of sand vented to the surface was sufficient to form a continuous sheet of sand 1 to 1.5 m thick. North of this sand sheet area and northeast of the point showing Nuttli's December 16 epicenter, there are only localized places where the vented sand is so thick and continuous. The center of the sand sheet area is about 50 to 60 km from the farthest margin of sand blow development, south of Marked Tree.

To be consistent with the definition of epicenter used for the Nuttli-Herrmann curves in figure 9, the midpoint of the energy release line must be used. The midpoint is determined by using a rupture (fault) length of 60 km for the December 16 earthquake (Nuttli, 1983). Adding half this length (30 km) to the distance from the southernmost possible limit of the energy release line to the boundary of sand blows (40–45 km) yields 70 to 75 km. Adding half the rupture length (30 km) to the distance from the center of the southern sand sheet to the southwestern boundary of sand blows (50–60 km) yields 80 to 90 km.

An independent assessment of this range of epicentral distances is provided by a study of possible epicenters for the February 7, 1812, earthquake. The epicentral region for this earthquake was probably somewhere in the area of the Lake County uplift (Russ, 1982). This uplift, structural in origin, extends from about 5 km north of New Madrid to 30 km south of New Madrid. The southern limit of the dome is coincident with intersecting north- and northeast-trending faults at a point about 25 km south of Reelfoot Lake (fig. 7). The southern limit of doming is also coincident with an area where vented sand coverage is exceptionally high (fig. 7).

The February 7 earthquake (M_S=8.8) was stronger than the December 16 earthquake (M_S=8.3–8.5), according to Nuttli (1984). Thus, the sand blows formed by the February 7 earthquake should presumably have been farther from the epicenter than those formed by the December 16 earthquake. The southern limit of doming is about 70 km from the northern limits of sand blows (south of Cairo). It is remotely possible that sand blows were formed in terrace deposits some few kilometers north of Cairo and that these sand blows have been covered by a veneer deposited by flooding since 1811–12. Even when this possibility has been accounted for, the southern limit of doming is not more than 85 km from the northern limit of sand blows.

Therefore, for the earthquake of December 16, an epicentral distance of 75 to 80 km seems reasonable. This "most reasonable epicenter" is shown as point C in figure 9.

The author believes that the most reasonable curve of acceleration as a function of epicentral distance, for m_b=7.1 (equivalent to M_S=8.5), goes through point C and is parallel to the curves for m_b=7.0 and m_b=6.5; point C is intended for both bedrock and medium thick (30–50 m), medium dense sand in the St. Francis Basin.

Also shown in figure 9 is a data point (C^1) that represents the upper bound of reasonable peak horizontal accelerations in bedrock the same distance from the epicenter as point C (75–80 km). The acceleration at C^1 is 0.25 *g*. This upper bound is based on the premise that the accelerations based on figure 5 may be as much as 25 percent too low. Even assuming that, for the December 16 earthquake, the peak acceleration at the border of sand blows may

possibly have been 20 percent lower than that in bedrock (on the basis of a study of bedrock-surface acceleration relations anticipated for Memphis by Sharma and Kovacs (1980)) yields an acceleration of 0.29 *g* at an epicentral distance of 75 to 80 km; this point in figure 9 (not shown) falls almost exactly on the Nuttli-Herrmann curve for m_b=7.1.

In summary, Nuttli and Herrmann's curves indicate accelerations that are higher than what can be accounted for by the liquefaction-based data. It also should be noted that the Nuttli-Herrmann relations in figure 9 are the average of two components. Liquefaction, however, is controlled primarily by the peak component of acceleration (Seed and others, 1975). Again, the Nuttli-Herrmann values seem a little too high.

Comparing predicted accelerations using the Nuttli-Herrmann curves with occurrences of farthest liquefaction (at St. Louis and along the Wabash River in southern Indiana) induced by the February 7 earthquake yields a similar conclusion. These two sites are in regions that represent the two most likely candidates for the focusing of energy and thus for the farthest occurrences of liquefaction (see fig. 12 for regions of focusing). Both St. Louis and the Wabash River sites are about 250 to 275 km from the center of the Lake County uplift. Using 250 to 275 km as epicentral distance and m_b=7.4 for the February 7 earthquake (Nuttli, 1983) and the Nuttli-Herrmann curves in figure 9 yields an acceleration of about 0.10 to 0.11 *g*. This base acceleration is estimated to be amplified by a factor of 1.5 in the thick alluvium near St. Louis (Higgins and Rockaway, 1986, p. 85). Thus, anticipated peak accelerations for the February 7 earthquake are 0.15 to 0.16 *g*. In contrast, using an N_1 value of 10 for flood plain deposits (because such low values are common) and the curve for M_S=8.5 in figure 5 conservatively yields a field cyclic stress ratio of 0.08. Equating this cyclic stress ratio to a typical field situation (using the equation on p. 6) yields an acceleration of 0.08 *g*. Clearly, the difference between the liquefaction model and the Nuttli-Herrmann curves is quite large (factor of two). It is possible that sand blows occurred even farther than 250 to 275 km from the February 7 epicenter, but, if the accelerations were as large as the Nuttli-Herrmann curves predict, sand blows and other types of liquefaction-related features in flood plain deposits at St. Louis or along the Wabash River should have been commonplace and quite large rather than hardly mentionable.

Because acceleration for the 1811–12 earthquakes indicated by the Nuttli-Herrmann curves in figure 9 is higher than that indicated by the liquefaction data, it is suggested that, for moderate to great earthquakes, the Nuttli-Herrmann curves be considered as the upper bound for liquefaction analysis. The set of curves would be for peak horizontal accelerations on bedrock. Then, by using the curves to determine the acceleration for the magnitude and epicentral distance in question and adjusting the accelerations for local ground conditions (such as thickness of alluvium and dynamic modulus properties), the liquefaction potential can be assessed from figure 5. This assessment would be for movement along the axis of a a strike-slip fault and thus would be an upper limit estimate of acceleration.

Magnitude Method

Both theoretical calculations (Youd and Perkins, 1978) and field observations of liquefaction features (Kuribayashi and Tatsuoka, 1975; Youd, 1977; Youd and Perkins, 1978; Davis and Berrill, 1983; Keefer, 1984) demonstrate a reasonably well defined relation between the farthest extent of significant liquefaction and the distance from the epicenter for a given earthquake magnitude and a fixed susceptibility to liquefaction. The field observations were predominantly in Holocene-age silt, silty sand, or sand, which are materials that typically have moderate to high susceptibility to liquefaction during strong shaking (Youd and Perkins, 1978).

Figure 10 shows results based on field observations and some suggested practical bounds on the limits of localized damaging liquefaction. The solid line is the outer limit of lateral spreads or flows, based on data by Davis and Berrill (1983) and by Keefer (1984)[5] from more than 46 earthquakes scattered around the world. (Keefer's compilation includes both natural deposits and artificial fill.) Very probably, most of these data are from sites where there was at least 40 mm of differential lateral movement, which is sufficient to damage structures that are very sensitive to deformation. Such structures include some underground pipes, concrete-lined canals, and poorly built buildings (especially old brick bearing-wall buildings). The dashed line is the best fit of data for all types of liquefaction-induced ground failure in Japan, including sand blows, reported by Kuribayashi and Tatsuoka (1975). The dotted line is, for practical purposes, the outer limit of liquefaction-induced ground failure on natural deposits from all data sources. Only rarely do data for natural deposits lie on the solid line, which shows the outer limit of reported data.

The curves (solid, dashed, and dotted) are for predominantly loose sediments, but the publications containing the data used to determine the curves do not report the

[5]The smallest displacements reported by Keefer are at least 40 mm; however, at least some (very few) data points that Keefer showed in his figures could have had smaller displacements (D.K. Keefer, personal communication, 1984). For these reasons, it is presumed that, for practical purposes, the lateral displacements were greater than 40 mm. In his original compilation, Keefer used moment magnitudes (M_W) for M>7.5; a replot of Keefer's data for figures 10 and 11 using surface-wave magnitudes (M_S) shows basically no change in the curve of the outer limit of reported data. Values of M_S for the replot of the 1811–12 earthquakes are from Nuttli (1983).

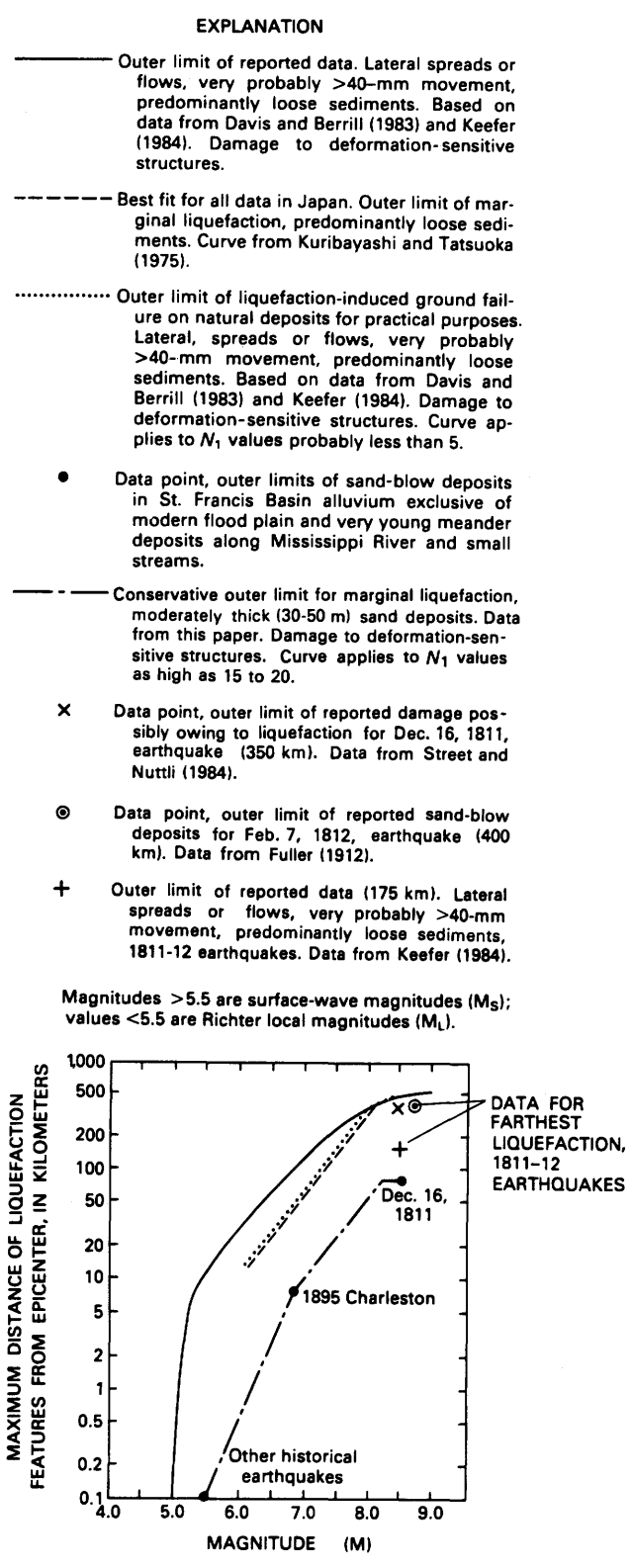

Figure 10. Maximum distance from the epicenter of liquefaction in sand as a function of earthquake magnitude (part of this figure is modified from data by Keefer (1984)).

thickness of sediments and possible bedrock acceleration amplifications. It is likely, though, that very considerable amplification (by a factor of 1.5 or more) occurred at many of the liquefaction sites.

Figure 10 also shows the liquefaction farthest from the 1811–12 earthquake epicenters. Three data points show the outer limit of damage possibly due to liquefaction, the outer limit of reported sand blows, and the outer limit of lateral spreads or flows. Figure 10 shows that, for the 1811–12 earthquakes, the outer limits of liquefaction did not extend an unusually large distance in comparison with those for other large earthquakes scattered around the world. This observation seems surprising at first, because of the huge area over which the 1811–12 earthquakes caused high MM intensities. It is possible that occurrences of sand blows and other liquefaction-induced features took place much further than 400 km from the epicenter (the farthest distance on fig. 10) and were not observed, but the author does not believe that to be the case. In 1811, there were many settlers in western Kentucky and along the Ohio River valley, which has a wide flood plain westward from the midlongitude of Indiana. This flood plain contains thick deposits of clean sand at many places. Natural levees along the Ohio River are generally small, low features, and sand blows caused by flooding are not commonplace. Surely, because they are unusual, sand blows caused by the 1811–12 earthquakes would have been noticed and reported. Instead, it is more likely that the alluvium in these flood plains is not as loose as that in many of the other localities exhibiting liquefaction in figure 10. Probably the only sediments having very high liquefaction susceptibility in the central Mississippi Valley region are modern sand bar deposits and very young point bar and abandoned meander deposits less than 500 years old; these deposits would be the only materials liquefied at the outer limits from the epicenters. The dotted line in figure 10 is, therefore, believed to be a practical outer limit for very loose sands in the central Mississippi Valley. Only sand deposits for which N_1 values are less than about 5 would be susceptible at this limit, on the basis of data compiled by Davis and Berrill (1983).

Figure 10 also shows a conservative outer limit for marginal liquefaction of alluvial deposits in the St. Francis Basin (and, by extension, in the Western Lowlands Basin as well); modern flood plain and very young deposits are excluded. These limits were determined by using distance C on figure 9 (75–80 km) as the maximum distance from the epicenter to the outer bound of liquefaction features for the December 16 earthquake (the author believes this distance to be conservative, because it is the distance on fig. 7 from the center of high-intensity sand blow development to the southwestward limit of sand blows). For the 1895 Charleston earthquake, the midpoint between the outer limits of sand blows is used as the distance from the epicenter; the Charleston data are based on a maximum diameter of 16 km for sand blows (based on information reported by Powell, 1975). The data from historical earthquakes in table 5

provide a third point at M = 5.5. The shape of the curve also has been chosen to be conservative. For magnitudes less than 8.2 and larger than 6.8, the slope is the same as that for much weaker sands; the overall shape conforms to that of the outer limit (solid) line. This curve, for the limits of marginal liquefaction, probably represents the outer limits at which liquefaction would cause some serious structural damage to poorly built, old commercial or residential brick or block buildings and other deformation-sensitive structures, but well-built masonry buildings and houses would experience only some cracking and other minor distressing. The curve applies to alluvial deposits at least 30 m thick and containing sand in which N_1 values as low as 15 to 20 are relatively common in the upper 10 m (for example, 2–3.5 m of sand deposits for which $N_1 < 15$–20).

For a large earthquake, as Youd and Perkins (1978) pointed out, epicentral distance is not a very good measure for the type of correlation shown in figure 10, because the epicenter does not define the entire zone of energy release. They suggested, therefore, that the seismic source zone (or fault rupture zone) is a better point of reference. A plot showing the maximum horizontal (map) distances of lateral spreads and flows from the fault rupture zone as given in reports by Keefer (1984) and Youd (1985) is the primary basis for figure 11. (Keefer's curve has been modified in accordance with comments by Youd.) Figure 11 shows the outer limits, for practical purposes, for lateral spreads and flows exhibiting more than 40 mm of movement in predominantly loose sediments (solid line) and the practical outer limit for marginal liquefaction in St. Francis and Western Lowlands Basins alluvium, exclusive of modern flood plain and very young deposits (long- and short-dashed line).

Fault rupture locations for the 1811–12 earthquakes were estimated from fault zones shown in figure 7. For the December 16 earthquake, the fault zone north of Marked Tree was used as the point from which to measure the farthest liquefaction, which was taken to be the outer bound of sand blows southwest of Marked Tree. For the February 7 earthquake, the fault zone at Reelfoot Lake was used as the reference point, and the farthest liquefaction was taken to be the northernmost bound of sand blows in the braided stream deposits between Sikeston Ridge and Crowleys Ridge. The fault rupture for the 1895 Charleston earthquake was the location central to the margin of sand blows.

The solid line in figure 11 is a conservative limit for potentially damaging liquefaction in natural loose deposits ($N_1 \leq 5$). This solid line should be used for the modern flood plain deposits and very young alluvium. The long-dash–short-dash line is thought to be a conservative bound for the alluvium in the St. Francis and Western Lowlands Basins, except for deposits on modern flood plains and very young alluvium.

APPLICATION OF METHODS

Both the Simplified Procedure of Seed and Idriss (used in conjunction with acceleration–epicentral distance

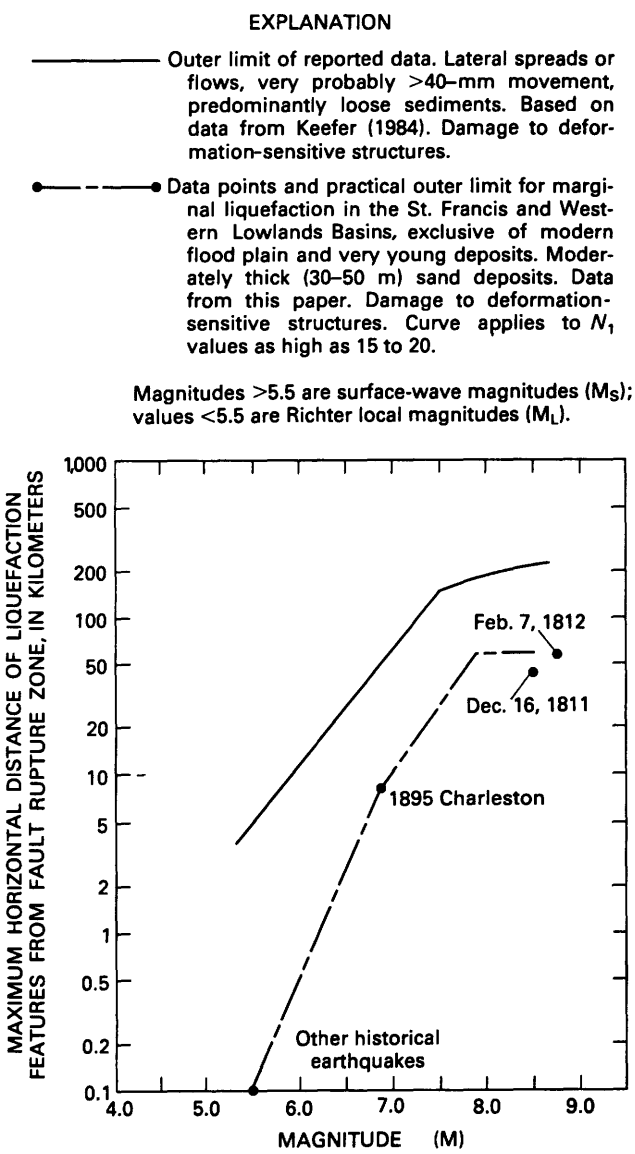

Figure 11. Maximum distance from fault rupture zone of liquefaction in sand as a function of earthquake magnitude (part of this figure is modified from data by Keefer (1984) and Youd (1985)).

curves in fig. 9) and the magnitude method are conservative approaches to estimating where liquefaction is likely to occur in that they overestimate the geographic region where potential liquefaction problems exist. Both methods show only the farthest limits, accounting for effects such as focusing of energy from the epicenter or source fault.

Focusing can cause a major distortion in the pattern of ground shaking, as the MM intensity contours in figures 8 and 12 illustrate. Figure 8 shows approximately average regional intensities for the December 16, 1811, earthquake; figure 12 is a possible maximum regional intensity map for an 1811-sized earthquake having an epicenter anywhere in the New Madrid seismic zone (that is, the zone of present intense microseismicity).

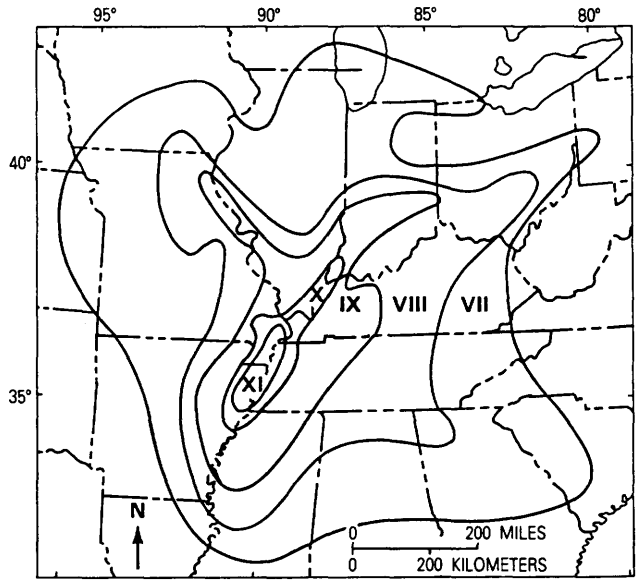

Figure 12. Possible regional intensity map (based on historic earthquake data) showing estimated Modified Mercalli intensity values for an 1811-sized earthquake ($M_S = 8.6$) having an epicenter anywhere along the New Madrid seismic zone (from Hopper and others, 1983). Intensity values are the highest that can be reasonably expected within an area. The seismic zone used to make the map corresponds approximately to the region of concentrated modern epicenters in southeastern Missouri, northwestern Tennessee, and northeastern Arkansas, reported by Stauder (1982).

Figure 12 is based on data from earthquakes listed in table 5. Intensity data from all the larger historical earthquakes (1811, 1843, 1895) having epicenters approximately in the zone of most frequent modern seismic activity (Stauder, 1982) (from approximately Marked Tree to Cairo) have MM intensity values of VII and higher and are consistently strongly focused in much the same geographic area. Hopper and others (1983) found that the largest MM intensities are in a region oriented approximately parallel to the zone of modern seismicity; in addition, there is some focusing in close proximity to the Mississippi River, extending from near Cairo toward St. Louis. Figure 12 was made by drawing MM intensity contour maps for the 1843 and 1895 earthquakes and then scaling them to the 1811 earthquake. For example, the highest MM intensity for the 1895 earthquake was VIII, and the highest for 1811 was XI; thus, a value of III was added to all the 1895 values. Intensity values in figure 12 approach being the highest that can be expected in a region, accounting for the influence of both focusing of energy and amplification of bedrock motions on weak soil.

Although figures 8 and 12 indicate that there are large variations in shaking severity as a function of distance from the epicenter, it does not now seem practical or realistic to try to quantify these variations on the basis of the two methods developed in this paper. Instead, it is suggested that estimates of the farthest limits of liquefaction be based both on the Simplified Procedure of Seed and Idriss in conjunction with figure 9 and on the magnitude method; in addition, reports published elsewhere on the relations between epicentral distance, MM intensity, and acceleration (for example, Nuttli and Herrmann, 1984a, b; Krinitzsky and Marcuson, 1983) should be consulted.

When MM intensity relations are used, it should be remembered that, for practical purposes, an average regional value of MM VII is the liquefaction threshold for modern flood plain deposits, which have very loose sands. On a map of maximum intensity values, such as figure 12, MM VIII is therefore the threshold for minor occurrences of liquefaction of very loose sediments subjected to highly amplified bedrock motion; for figure 12, MM IX is probably the intensity threshold at which damaging liquefaction becomes relatively commonplace in very loose to loose sands. The MM values shown for much of the area in figure 12 are two units higher than average regional MM values, such as those shown in figure 8.

The final judgment on whether potential problems exist must be based on the consequences of an occurrence of liquefaction. For example, if all methods show that a high probability of liquefaction exists and if a critical structure is involved, then some sort of mitigation is in order. For other than critical structures, the decision may be quite subjective.

LIQUEFACTION SUSCEPTIBILITY AND GEOLOGIC ORIGIN

The texture, mode of deposition, and age of deposits affect liquefaction potential in a generally predictable way (Youd and Perkins, 1978), as discussed earlier. On the basis of these criteria, sediments in the central Mississippi Valley have been categorized for susceptibility to liquefaction on a regional basis (at a scale of 1:1,000,000) by means of surficial geologic map units (Obermeier and Wingard, 1985). Surficial geologic maps are available in all States at a scale of 1:1,000,000 and, in some States, at scales showing much more detail. Maps at a scale of 1:62,000 or 1:24,000 are optimal but are generally available only for localized areas.

Because many of the deposits shown on the State maps have formation names that may change at a State boundary, names are not used in this discussion; rather, the geologic origin and age are used as a basis. Liquefaction potential is given in terms of N_1 values whenever possible.

Braided Stream and Meander Belt Deposits

The properties of Wisconsinan-age glacial outwash (braided stream) deposits and those of Mississippi River

meander belt deposits, shown in figure 2, have been described previously in the text and in table 4 and will only be summarized here. Median N_1 values are generally near 25 in the upper 15 m and increase slightly with depth. Rarely, N_1 values are as low as 10 to 12 within the upper 15 m. There are abundant thick, clean sands that fine upward to a thin stratum of fine or silty sand just beneath a clay-rich cap, which is generally 3 to 6 m thick. Glaciofluvial terrace deposits possessing about the same properties are present along many of the larger streams north of the St. Francis Basin. The Wabash and Ohio Rivers have especially large volumes of clean sand in Illinois and Indiana. Thicknesses of 30 m are not unusual.

Although rivers farther south did not carry glacial outwash, many have terraces that are Late Wisconsinan in age or older and are composed dominantly of thick, clean sands. The Obion River in Tennessee has some especially large terraces. The terrace deposits along the southern rivers probably have about the same resistance to liquefaction as the braided stream deposits in the St. Francis and Western Lowlands Basins do, because they are all about the same age, contain minerals having about the same physical properties, and have shallow water tables.

Glacial Lake Deposits

Large glacial lakes formed along many rivers carrying glacial meltwater, particularly in Indiana, Illinois, and Kentucky. Many of these glacial lakes laid down thick deposits of sand, silt, and clay. At many places, grain size tends to fine upward from a basal sand. Thicknesses of 15 m are commonplace.

Near large streams, thick and unusually loose sands ($N_1 \approx 8$) about 6 m deep occur at many places. Elsewhere, the sands are denser and have much higher N_1 values. Very soft silts and clayey silts having SPT blow counts of 2 to 3 are relatively common in low terraces adjoining streams throughout Indiana, Illinois, and Kentucky. The higher, better drained terraces typically have much higher blow counts owing to the effects of dessication and a lower ground-water table.

Modern Flood Plain Deposits, Exclusive of Very Young Sediments

Very young sediments less than about 500 years old are excluded from the class of modern flood plain deposits. Modern flood plains along major streams generally have thick strata of clean sand, silt, and clay. The sands generally have median N_1 values of 15 that are commonplace locally. Silt-rich strata in some abandoned channels are so soft as to be potentially subject to liquefaction.

Very Young Sediments

Very young sediments are defined as being less than 500 years old. Very young sediments typically border streams as point bars or are sand bars in streams. However, very young meander cutoffs can be far from large streams. N_1 values of less than 10 are very common in sands. Very young meander cutoffs also contain very loose, very soft sediments at many places.

Eolian Deposits

Thick loess deposits are found in many upland areas near major streams that carried large volumes of glacial meltwater. The Wabash and Mississippi Rivers have especially thick loess deposits on uplands adjoining the flood plain, especially east of the rivers. Near the rivers, thicknesses of 20 to 25 m are not unusual. The loess is predominantly silt and exhibits almost no cohesion at some places. Even clayey silt loess can have an extremely low cohesion and a sensitivity[6] as high as 10 and is possibly subject to liquefaction under conditions of large shear straining or flowing (Randall Jibson, oral communication, 1984), although landslides in loess caused by the 1811–12 earthquakes have no features indicative of large flowage. Locally, and especially near large rivers, loess has lenses of clean, very loose dune sand or water-deposited strata of clean sand. In the highly dissected upland areas of thick loess, the loess may be only locally or partially saturated far beneath the ground surface and is not very susceptible to liquefaction except very locally. Where the ground water table is high, though, it is possible that slopes in loess are potentially subject to flowing failure during earthquakes.

Reworked Eolian Deposits

At the base of the high loess bluffs along major rivers, there is generally a veneer of silt washed down from the hills. This veneer is 6 m thick at many places and is commonly very soft in lowland areas. Clearly, many of these sediments are weak enough to liquefy in moderate to severe shaking, although liquefaction would probably be accompanied by limited straining in most cases. To the author's knowledge, the only data relevant to evaluation of dynamic behavior of reworked eolian materials are in a thesis by Puri (1983).

SUMMARY

There are so few data on strong earthquakes in the central Mississippi Valley that each of the methods most

[6]Sensitivity is defined as the ratio of undisturbed unconfined compressive strength divided by the remolded unconfined compressive strength.

commonly used for evaluating liquefaction potential, whether it is based on accelerations, magnitudes, or intensities, has some uncertainty. However, on the basis of production of earthquake-induced liquefaction during the 1811–12 earthquakes, the Nuttli-Herrmann curves showing relations between acceleration and epicentral distance are conservative for engineering analysis. Conservative bounds have also been established for farthest liquefaction in many geologic settings for different earthquake magnitudes.

There are many large terraces and flood plains in the central Mississippi Valley region that contain moderately dense to loose clean sands and silty sands. Evaluation of their liquefaction potential is reasonably easy and straightforward.

Many thick glacial lake deposits, eolian deposits, and reworked eolian deposits are made up of silt-rich materials of generally low but locally high liquefaction susceptibility. Even if the silt-rich materials are liquefied, however, it is likely that their capacity for large straining is limited. Field methods for assessing their liquefaction susceptibility are extremely crude at best, and laboratory data appear to be so scarce that there are no guidelines based on simple criteria such as void ratio, cohesion, and plasticity characteristics.

REFERENCES CITED

American Society for Testing and Materials, 1978, Annual book of ASTM standards, pt. 19, Designation D 1586–67 (reapproved 1974), standard method for penetration test and split barrel sampling of soils: Philadelphia, Pa., p. 235–237

Anderson, L.R., Keaton, J.R. Aubry, K., and Ellis, S.J., 1982, Liquefaction potential map for Davis County, Utah: Salt Lake City, Utah, Dames and Moore Consulting Engineers, 49 p.

Bennett, M.J., Youd, T.L., Harp, E.L., and Wieczorek, G.F., 1981, Subsurface investigation of liquefaction, Imperial Valley earthquake, California, October 15, 1979: U.S. Geological Survey Open-File Report 81–502, 83 p.

Coffman, J.J., and von Hake, C.A., 1973, Earthquake history of the United States: National Oceanic and Atmospheric Administration Publication 41–1, 208 p.

Davis, R.O., and Berrill, J.B., 1983, Comparison of a liquefaction theory with field observations: Geotechnique, v. 32, no. 4, p. 455–460.

Fuller, M.L., 1912, The New Madrid earthquake: U.S. Geological Survey Bulletin 494, 119 p.

Hamilton, R.M., and Zoback, M.D., 1982, Tectonic features of the New Madrid seismic zone from seismic reflection profiles, *in* McKeown, F.A., and Pakiser, L.C., eds., Investigations of the New Madrid, Missouri, earthquake region: U.S. Geological Survey Professional Paper 1236-F, p. F55-F82.

Higgins, J.D., and Rockaway, J.D., 1986, A graphics system for seismic response mapping: Bulletin of the Association of Engineering Geologists, v. 23, no. 1, p. 77–91.

Hopper, M.G., Algermissen, S.T., and Dobrovolny, E.E., 1983, Estimation of earthquake effects associated with a great earthquake in the New Madrid seismic zone: U.S. Geological Survey Open-File Report 83–179, 94 p.

Housner, G.W., 1958, The mechanism of sandblows: Bulletin of the Seismological Society of America, v. 48, p. 155–161.

Ishihara, K., 1985, Stability of natural deposits during earthquakes, *in* International Conference on Soil Mechanics and Foundation Engineering, 11th, San Francisco 1985, Proceedings: Boston, Balkema, v. 1, p. 321–376.

Keefer, D.K., 1984, Landslides caused by earthquakes: Geological Society of America Bulletin, v. 95, p. 406–421.

Krinitzsky, E.L., and Marcuson, W.F., 1983, Principles for selecting earthquake motions in engineering design: Bulletin of the Association of Engineering Geologists, v. 20, no. 3, p. 253-265.

Kuribayashi, E., and Tatsuoka, F., 1975, Brief review of liquefaction during earthquakes in Japan: Soils and Foundations, v. 15, no. 4, p. 81–92.

Mosaic, 1979, When soils start to flow: v. 10, no. 4, p. 26–34.

Nicholson, C., Simpson, D.W., Singh, S., and Zollweg, J.E., 1984, Crustal studies, velocity inversions, and fault tectonics: Results from a microearthquake survey in the New Madrid seismic zone: Journal of Geophysical Research, v. 89, no. B6, p. 4545–4558.

Nuttli, O.W., 1979, Seismicity of the central United States, *in* Hatheway, A.W., and McClure, C.R., Jr., eds., Geology in the siting of nuclear power plants: Reviews in Engineering Geology, v. 4, p. 67–93.

———1981, Evaluation of past studies and identification of needed studies of the effects of major earthquakes occurring in the New Madrid fault zone: Report submitted to Federal Emergency Management Agency, Region VII, Kansas City, Mo., 28 p.

———1983, Empirical magnitude and spectral scaling relations for mid-plate and plate-margin earthquakes, *in* Duda, S.J., and Aki, K., eds., Quantification of earthquakes: Tectonophysics, v. 93, nos. 3–4, p. 207–223.

Nuttli, O.W., and Herrmann, R.B., 1978, State-of-the-art for assessing earthquake hazards in the United States—Credible earthquakes for the Central United States: U.S. Army Corps of Engineers Miscellaneous Paper S-73–1, Report 12, 99 p.

———1982, Earthquake magnitude scales: American Society of Civil Engineers Proceedings, Journal of the Geotechnical Engineering Division, v. 103, no. GT 5, p. 783–786.

———1984a, Ground motion of Mississippi Valley earthquakes: Journal of Technical Topics in Civil Engineering, American Society of Civil Engineers, v. 110, v. no. 1, p. 54–69.

———1984b, Source characteristics and strong ground motion of New Madrid earthquakes, *in* Gori, P.L., and Hays, W.W., eds., Proceedings of the symposium on the New Madrid seismic zone: U.S. Geological Survey Open-File Report 84–770, p. 330–352.

Obermeier, S.F., in press, The New Madrid earthquakes: An engineering-geologic interpretation of relict liquefaction features: U.S. Geological Survey Professional Paper 1336-B.

Obermeier, S.F., and Wingard, N.E., 1985, Potential for liquefaction in areas of Modified Mercalli intensities IX and greater, *in* Hopper, M.G., ed., Estimation of earthquake effects associated with large earthquakes in the New Madrid seismic zone: U.S. Geological Survey Open-File Report 85-457, p. 127–140.

Obermeier, S.F., Jacobson, R.B., Powars, D.S., Weems, R.E., Hallbick, D.C., Gohn, G.S., and Markewich, H.W., 1986, Holocene and late Pleistocene(?) earthquake-induced sand blows in coastal South Carolina, *in* U.S. National Conference on Earthquake Engineering, 3d, Charleston, S.C., 1986, Proceedings: El Cerrito, Calif., Earthquake Engineering Research Institute, v. 1, p. 197–208.

Powell, B.F., 1975, History of Mississippi County, Missouri, beginning through 1972: Independence, Mo., BLN Library Service.

Puri, V., 1983, Liquefaction behavior and dynamic properties of loessial (silty) soils: Rolla, Mo., University of Missouri, unpublished Ph.D. thesis, 295 p.

Russ, D.P., 1982, Style and significance of surface deformation in the vicinity of New Madrid, Missouri, *in* McKeown, F.A., and Pakiser, L.C., eds., Investigations of the New Madrid, Missouri, earthquake region: U.S. Geological Survey Professional Paper 1236-H, p. H95-H114.

Saucier, R.T., 1964, Geological investigation of the St. Francis Basin, lower Mississippi Valley: U.S. Army Corps of Engineers Waterways Experiment Station Technical Report 3–659.

———1974, Quaternary geology of the lower Mississippi Valley: Arkansas Archeological Survey Research Series, no. 6, 26 p.

———1977, Effects of the New Madrid earthquake series in the Mississippi alluvial valley: U.S. Army Corps of Engineers Waterways Experiment Station Miscellaneous Paper S-77–5, 10 p.

Seed, H.B., 1968, Landslides during earthquakes due to soil liquefaction: Proceedings of the American Society of Civil Engineers, Journal of the Soil Mechanics and Foundations Division, v. 93, no. SM5, p. 1055–1122.

———1979, Soil liquefaction and cyclic mobility for level ground during earthquakes: Proceedings of the American Society of Civil Engineers, Journal of the Geotechnical Engineering Division, v. 105, no. GT2, p. 201–255.

Seed, H.B., and Idriss, I.M., 1971, Simplified procedure for evaluating soil liquefaction potential: Proceedings of the American Society of Civil Engineers, Journal of the Soil Mechanics and Foundations Division, v. 93, no. SM9, p. 1249–1273.

———1982, Ground motions and soil liquefaction during earthquakes: Berkeley, Calif., Earthquake Engineering Research Institute Monograph Series, 134 p.

Seed, H.B., Idriss, I.M., and Arango, I., 1983, Evaluation of liquefaction potential using field performance data: Proceedings of the American Society of Civil Engineers, Journal of the Geotechnical Engineering Division, v. 109, no. GT3, p. 458–482.

Seed, H.B., Idriss, I.M., Makdisi, F., and Bannerjee, N., 1975, Representation of irregular stress time histories by equivalent uniform stress series in liquefaction analyses: Berkeley, Calif., Report EERC 75–28, Earthquake Engineering Research Center, University of California, 13 p.

Sharma, S., and Kovacs, W.D., 1980, Microzonation of the Memphis, Tennessee, area: West Lafayette, Ind., Purdue University, Report 14–08-0001–17752, 129 p.

Smith, F.L., and Saucier, R.T., 1971, Geological investigations of the Western Lowlands area, lower Mississippi Valley: U.S. Army Corps of Engineers Waterways Experiment Station Technical Report S-71–5.

Stauder, W., 1982, Present day seismicity and identification of active faults of the New Madrid seismic zone, *in* McKeown, F.A., and Pakiser, L.C., eds., Investigations of the New Madrid, Missouri, earthquake region: U.S. Geological Survey Professional Paper 1236-C, p. C21-C30.

Street, R.L., and Nuttli, O.W., 1984, The central Mississippi Valley earthquakes of 1811–12, *in* Gori, P.L., and Hays, W.W., eds., Proceedings of the symposium on the New Madrid seismic zone: U.S. Geological Survey Open-File Report 84–770, p. 33–63.

Terzaghi, K., and Peck, R.B., 1967, Soil mechanics in engineering practice: New York, John Wiley, 566 p.

Tokimatsu, K., and Yoshimi, Y., 1981, Field correlation of soil liquefaction with SPT and grain size: International Conference on Recent Advances in Geotechnical Earthquake Engineering and Soil Dynamics, Rolla, Mo., 1981, Proceedings, v. 1, p. 203–208.

Youd, T.L., 1973, Liquefaction, flow, and associated ground failure: U.S. Geological Survey Circular 688, 12 p.

———1977, Discussion of brief review of liquefaction during earthquakes in Japan by Eiichi Kuribayashi and Fumio Tatsuoka, 1975: Soils and Foundations, v. 17, no. 1, p. 82–85.

———1978, Major cause of earthquake damage is ground failure: Civil Engineering, v. 48, no. 4, p. 47–51.

———1985, Landslides caused by earthquakes: Discussion: Geological Society of America Bulletin, v. 96, p. 1091–1092.

Youd, T.L., and Bennett, M.J., 1983, Liquefaction sites, Imperial Valley, California: Proceedings of the American Society of Civil Engineers, Journal of the Geotechnical Engineering Division, v. 109, no. GT3, p. 440–457.

Youd, T.L., and Hoose, S.N., 1978, Historic ground failures in northern California triggered by earthquakes: U.S. Geological Survey Professional Paper 993, 177 p.

Youd, T.L., and Perkins, D.M., 1978, Mapping liquefaction-induced ground failure potential: Proceedings of the American Society of Civil Engineers, Journal of the Geotechnical Engineering Division, v. 104, no. GT4, p. 433–446.

☆ U.S. GOVERNMENT PRINTING OFFICE: 1988 - 201-933 - 226/80025